Universidad Nacional Autónoma de México

Centro de Nanociencias y Nanotecnología

Entanglement harvesting of three Unruh-DeWitt detectors

T E S I S

que para obtener el título de:

Licenciada en Nanotecnología

presenta:

Diana Méndez Avalos

Tutor:

Prof. Robert B. Mann

University of Waterloo

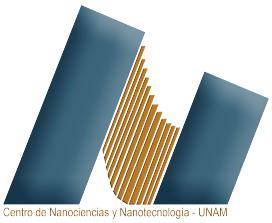

Ensenada, Baja California 2021

Hago constar que el trabajo que presento es de mi autoría y que todas las ideas, citas textuales, datos, ilustraciones, gráficas, etc. sacados de cualquier obra o debidas al trabajo de terceros, han sido debidamente identificados y citados en el cuerpo del texto y en la bibliografía y acepto que en caso de no respetar lo anterior puedo ser sujeto de sanciones universitarias. Afirmo que el material presentado no se encuentra protegido por derechos de autor y me hago responsable de cualquier reclamo relacionado con la violación de derechos de autor.

Diana Méndez Avalos

A mis padres Alejandra y Rodolfo me han enseñado
y que han confiado en mi y en mis capacidades
para poder volar lejos y llegar hasta donde yo quiera...

Acknowledgement

First, I want to thank my supervisor Prof. Robert Mann and my colleague and advisor PhD. Laura Henderson. Thank you both for your patience and your guidance during this process. You always make my time with you very comfortable and warm. In addition, I want to thank PhD. Allison Sachs for explaining to me the fundamental questions I got in Quantum Information, I admire your hability to explain the concepts so easily. I also want to thank Prof.Mann's group for teaching me a lot every session with all the discussions. I learned a lot from you all and it felt great!

I want to thank Dr. Fernando Rojas for your guidance during my previous work under your supervision. Thank you for receiving me even though I was a freshman at the beginning and for talking to me as if I was a master's student, I really appreciated it.

Thank you Gaby Rojas for believe in me and in all the Mexican Talent, with your unconditional support we will return all our work to Mexico very soon.

I want to thank my friends for being there always, in the best and in the worst. In particular, I want to thank Alma Sanchez, Kevin M. McManus, Denisse Rojas, Mauricio Carrasco and José Lucatero for being there since the beginning, for the good times and the most spectacular projects ever, you all are my inspiration every day and I love you and admire you a lot. It has been a pleasure grow by your side. To my babies Zarco, Dany, Paco, Xavier, Aylin, Mary, Demian, Paola, Ariel, Vera, I love you and admire you all, keep with your good vibes and always follow your dreams.

Thanks to my family, for always believe in me, for love me beyond everything and for being there always with all your hugs. Aunties Cristina and Irma, I love you both a lot, thank you

for your best wishes everytime. Grandma Maricarmen and Ana María Fabre, you are my role models, I love you very much. Roger, Katya and Tzeitel, thank you for all your advices and support. And to Plankis for being the cutest cat in the world.

I also want to thank all my life's teachers. Dr. Alejandro Ayala, Ing. Eduardo Murrieta, Dra. Rocío Jauregui, Mtro. Julio Hernández. Thank you all for listen and answer all the questions I had, and thank you for introducing me to the marvellous world of research.

Mom, dad, I have no words to describe how much I thank you for your support and unconditional love, your teachings and your understanding. I have become who I am today because of you. I promise one day I will be prudent, just kidding.

Last but not least, I want to specially thank Dante Serrano for your support in all the process. Thank you for your time, your love and for being my partner in crime. I will always love our long chats about everything, from the smallest thing to the most complicated science concepts we find. I love you.

Contents

List of Figures

Chapter 1

Introduction

Technology has come to change the way we live. Since the first industrial revolution, technology has advanced exponentially. Now, with the development of semiconductors, we are living the third industrial revolution. However, another one comes involving the recent flourishing of artificial intelligence, internet of things, nanotechnology, and quantum technologies such as quantum computing, quantum cryptography, quantum information, among others. Even though these technologies are still under development, they represent a massive change in the economic, social, and technological sector [1].

Most of the basis of these new technologies came with revolutionary ideas of the 20th century. To be specific, the birth of quantum mechanics as a new branch of physics changed some fundamental concepts that are used today to develop the present and the future's technology.

Furthermore, the most spectacular and counter-intuitive concept of quantum mechanics is entanglement. This is the property where two or more particles depend on each other to determine their state in space and time; also, it cannot be written as a separable state. The entanglement in quantum systems has significant consequences, as entangled particles remain connected. In other words, the actions performed on one affect the other, even when they are separated by great distances. Besides, entanglement ended up being foundational for one of the major branches of quantum physics, the modern field of quantum information science.

Quantum information focuses on how we can send and receive information better and faster

using quantum properties of particles, and it can be a paradigm shift of how it has been done classically. This science has evolved significantly over the last 20 years, since quantum field theory became essential to explain multiple quantum phenomena, from condensed matter to high energy physics, and more recently, quantum-relativistic effects [2]. In fact, some of the greatest revolutions in physics in the 21st century involve this latter case.

For example, the leading investigations on the interface of quantum mechanics and relativity came with a whole new field, often referred to as relativistic quantum information [3, 4]. This area has potential applications related to the creation of new information protocols, and it is a plausible way to answer some of the fundamental questions about the quantization of gravity [5, 6]. These applications are one step further in the development of quantum technologies.

One of the most critical tools in relativistic quantum information is the Unruh-DeWitt detector, a theoretical particle-like model of two energy levels. This detector interacts with a quantum field through a function that changes the energy level in which the particle exists. In this way entanglement can be extracted from the quantum field. The explanation of this last phenomenon is that the ground state of a quantum field contains entanglement between different regions of space-time. This entanglement persists even for regions that are spacelike separated. Moreover, two uncorrelated detectors that interact with a quantum field can get entangled. In this way, the field entanglement can be harvested in the same way that a farmer harvests a crop of wheat. In other words, the entanglement of two or more regions of the quantum vacuum can be quantified by measuring the entanglement of the Unruh-DeWitt detectors.

As there has to be a certainty that entanglement has been created, mainly in experiments, there has to be a way to quantify entanglement. Nowadays, there are many methods and criteria to measure entanglement for different types of systems. Nevertheless, the bigger the system and the greater the number of variables, the more complicated it is to compute entanglement. In order to assess entanglement in tripartite states, there are two important entanglement measures: the Three-tangle and the π-tangle, or the Three-π [7]. The difference between them is the criteria for entanglement they use and the systems in which they can be used. These two measures have been useful in many cases, however, there needs to be more research on their limits in order to assure that they are valid for the conclusions to be trustworthy.

Moreover, there have been some developments on multipartite entanglement in different kinds of systems and some in entanglement harvesting with only two Unruh-DeWitt detectors. However, there is little information in the literature about extracting multipartite entanglement from the quantum vacuum with Unruh-DeWitt detectors. Now our question is: How much multipartite, and specifically tripartite, entanglement is present in a quantum field with three uncorrelated detectors?

Furthermore, it has been observed that in systems of two detectors there is a dependency on the separation. In other words, the closer they are, the greater is the quantity of entanglement that can be extracted. It would be intuitive to think that there is a dependency on the separation of three detectors so that the closer the detectors are, the greater the entanglement. One of the main goals of the present thesis work is to evaluate the entanglement's dependency on the detectors' separation and their energy gap in a tripartite system with the π-tangle as an entanglement measurement.

The thesis is presented as a partial fulfillment of the requirements to obtain a B.Sc in Nanotechnology from the Center of Nanosciences and Nanotechnology from the National Autonomous University of Mexico. The thesis is divided into five general chapters. The intention of the present one is to show an introduction to the thesis work. Chapter 2 exposes the background that will be useful to understand the precedents of the research and the importance, relevance and the fulfilment we want to accomplish. Chapter 3 presents the theoretical concepts and definitions of quantum mechanics and quantum field theory on which the work is built; besides the theoretical methodology of Unruh-DeWitt detectors that has been followed. The results of the triangle and linear alignment are shown in chapter 4 along with the discussions of the findings and further work. And finally, chapter 5 presents the conclusions of this thesis project. The references and appendices are at the end of the document.

Chapter 2

Background and Research Problem

2.1 Background

The idea of quantum technologies was born more than a century ago with the change of paradigm in physics, from classical to quantum, that changed how the universe is understood. Quantum physics emerged by the end of the 19th century when the experiments did not agree with physicists' theories, who tried to explain that radiation and matter have both characteristics of particles and waves.

First, there was the notion that light was a particle, called a corpuscle, was based on Newton's ideas. Later, the notion that light is a wave was finally accepted when Young's experiment showed that light created interference patterns as waves. However, the mathematical theories of the black body radiation problem did not agree with the empirical evidence. A hypothetical ideal black body absorbs, and reemits all radiant energy falling on it. The hypothesis was that temperature should always increase with the wavelength. Instead, physicists observed a curve that increased in temperature at low wavelengths, and decreased at high wavelengths. Then, Max Planck proposed that the radiation energy was emitted in discret packets, which he called quanta, the energy was quantized. After that, Einstein followed that idea proposing the explanation of the photoelectric effect, in which metals irradiated electrons after the incidence of light. Therefore, light behaves as both a wave and a particle. These developments introduced

a new area of physics called quantum mechanics as a new interpretation of physics.

On the other hand, the familiar and classical idea of the vacuum is the absence of particles, so the particle field is at its lowest energy state. This notion is strictly associated with physical particles and finite-amplitude fields. However, in quantum physics, the interpretation of the vacuum is quite different as the properties are not rigorously tied to objects. Instead, vacuum is defined as the ground state of a quantum field. It is a state of minimum energy, corresponding to zero particles [8]. Nevertheless, in his book “Relativity", Einstein agreed with Descartes and his belief that the existence of empty space must be excluded, as space-time claims its existence only as a structural quality of the field. Thus, there is no such thing as an empty space or a space without field [9].

As stated in the previous chapter, one particular manifestation of quantum mechanics is entanglement. It can be described as the property in which two or more particles depend on each other to determine their state in space and time. One of the characteristics of entanglement is that a state cannot be written as a separable state. Hence, there can be two types of states: entangled or separable. Along with this idea, there is another independent category of types of states: pure and mixed. Both can be either entangled or separable. On the one hand, the pure separable states can be expressed as a product of vector states $|\psi\rangle = \left|\phi^A\right\rangle \otimes \left|\phi^B\right\rangle$, where $\left|\phi^D\right\rangle$ is a state on the Hilbert space $\mathcal{H}_D$. On the other hand, a mixed state is separable if there are convex weights p_i and product states $\rho_i^A \otimes \rho_i^B$ such that $\rho = \sum_i p_i \rho_i^A \otimes \rho_i^B$, where ρ_i^D is a density matrix on the Hilbert space $\mathcal{H}_D$. Otherwise, both are entangled. In other words, a state is said to be entangled if it cannot be expressed as a tensor product of two or more different states [10].

Indeed, entanglement is not an intuitive idea. In fact, in 1935, Einstein, Podolsky, and Rosen (EPR) did not agree with the concept of entanglement. They showed that quantum theory leads to a contradiction if these two assumptions are correct [11]:

1) Reality principle: If we can predict the value of a physical quantity with certainty, then this value has a physical reality, independently of our observation.

2) Locality principle: If two systems are causally disconnected, the result of any measurement performed on one system cannot influence the result of a measurement performed on the second

system.

Einstein, Podolsky, and Rosen proposed the paradox in which it is not possible to assess that a quantum system has a given property before having measured it. Their conclusion to this paradox was that quantum mechanics is an incomplete theory. Later, the suggestion was that any measurement is a deterministic process, however, it appears probabilistic since some variables are not precisely known [11].

Furthermore, quantum entanglement is a critical resource that allows for performing basic quantum tasks in quantum information processing such as teleportation and quantum key distribution, which are impossible in the classical world [12].

Along with quantum mechanics, another radical change of paradigm in the 19th century was relativity, proposed by Albert Einstein. With his theories of special and general relativity, Einstein redefined the fundamental concepts of space, time, matter, energy, and gravity. On the other hand, Einstein established two main postulates that formed special relativity. The first postulate states that light has a constant speed for all observers in inertial frames of reference. The second postulate states that the laws of physics have to be the same form for all observers [13]. To make the first statement true, Einstein replaced absolute space and time with new definitions that depend on the state of motion of an observer. It was these two postulates that led Einstein to implement new equations of space and time which are called “the Lorentz transformations", as it was Hendrik Lorentz who first proposed them [14]:

$$x' = \frac{x - vt}{\sqrt{1 - \frac{v^2}{c^2}}}$$
$$t' = \frac{t - \frac{vx}{c^2}}{\sqrt{1 - \frac{v^2}{c^2}}}$$

where t' is time as measured by the moving observer; c is the speed of light; x indicates the distance between an event and a stationary observer, x' indicates the distance between the same event and a moving observer, and v is the moving observer's velocity.. However, Einstein noted that a particular combination of distance (D) and time interval (T), the quantity $D^2 - c^2T^2$, has the same value for all observers, which the invariant quantity cT turns time to a kind of mathematical parity with space [1]. Noting this, Hermann Minkowski showed that the universe resembles a four-dimensional structure. Later, Minkowski introduced the Minkowski space-time

diagram which is a geometric interpretation of the Lorentz transformation in which the motion of a particle may be regarded as a curve in a three-dimensional space and one-dimensional time together [15]. Hence, the universe can be described as a four-dimensional space-time continuum, a central concept in general relativity.

On the other hand, Einstein developed general relativity as a way to understand gravitation, since Newton's theory cannot be conceptually reconciled with special relativity. The basic idea of general relativity relies on the principle that *"on a local scale, meaning within a given system, without looking at other systems, it is impossible to distinguish between physical effects due to gravity and those due to acceleration"*[13], which is called the equivalence principle. With this principle then light must be affected by gravity as well [1]. This was a hint that gravity should be treated as a geometric phenomenon which led to the now well-known analogy of the sheet. This analogy begins by considering space-time as a rubber sheet that can be deformed and if there is a presence of a massive body such as bowling ball placed on the rubber sheet then it creates a depression which will make a marble placed near the depression roll down as if it is pulled by a force. Therefore, Einstein's theory of general relativity states that space-time geodesics define the deflection of light and the orbits of planets.

After Einstein developed relativity, he supported the idea of a unified theory that encompasses all the fundamental theories. Unfortunately, he failed in this task. However, other theorists have attempted to merge general relativity with quantum theory, but there has not been a successful theory yet. Nevertheless, there are some advances with the interaction between quantum mechanics and special relativity which lead to the so called quantum-relativistic effects that focus more in the interaction of space-time, time dilatation, changes of reference frames, among others.

The intersection of these two branches developed an entire area of study: quantum theory. This later gave the basis for one of the most important pieces of quantum technologies: quantum information. The main implications of the latter, are creating novel measurement protocols and answering fundamental questions about the quantization of gravity. This led to a new field, often referred as relativistic quantum information.

One of the basic theoretical models of relativistic quantum information is the Unruh-DeWitt

detector. The necessity, concept, and current applications of this kind of detector will be described as follows.

An observer with constant proper acceleration can detect thermal radiation in the quantum vacuum in a Minkowski space-time. This effect is called the Unruh-Davies effect. It was initially proposed as an alternative possibility of observing the thermal radiation coming from a black hole. Both effects are a result of the presence of an horizon in the space-time.

Unruh-DeWitt detectors provide an idealized mechanism for observation of these effects. These detectors are two-level systems that behave like a particle in a "box", which interacts with the field when the "box" opens. These detectors will be excited by the quantum field when they pass through it (See Fig.2.1). Such detectors represent an idealization of atoms responding to an electromagnetic field.

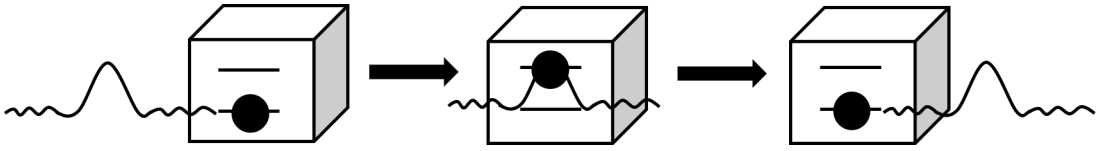

Figure 2.1: UDW detector diagram

In the 1990's Valentini [16], and a decade later Reznik [17, 18] discovered that the vacuum entanglement could be extracted from different regions of the field through the Unruh-DeWitt detectors. In fact, the relativistic quantum information sees the problem from the detector perspective and its local interactions with the field, which is a more operational approach than seeing only the field interaction. This idea opens the possibility of performing experiments by coupling a physical detector, such as an atom, qubit, photon, among others to the electromagnetic field [19].

One of the applications of this kind of detector is the quantification of a quantum field entanglement. As the Unruh-DeWitt detectors interact with the field, the amount of entanglement can be measured through the Unruh-DeWitt detectors.

The way entanglement can be measured depends on the properties of the system. There are some criteria of separability that tell if the state is entangled. One of the most crucial criteria

is the Positive Partial Transposition (PPT) criterion, or the Perez-Horedeki criterion, which is a solid indicator for entanglement [20]. This criterion states that if the partial transpose of a density matrix has at least one negative eigenvalue then the system is entangled [21]. Even though this criterion is very useful, it can fail in some cases when the eigenvalues are zero, which may happen if the density matrix has been approximated in some way.

For this latter problem, there have been some mathematical developments proposing many other criteria, such as the Computable Cross Norm or Realignment (CCNR) criterion, the range criterion, the majorization criterion, among others [10]. Some of these criteria use the Schmidt Decomposition or the Generalized Schmidt Decomposition (GSD) to evaluate the separability of the state[22]. However, these criteria also fail in some cases with multipartite states [23].

Since it has been shown that bipartite entanglement can be extracted from a quantum field [24, 25], several articles have been written based on this idea. For example, it has been shown that Unruh-DeWitt detectors can extract an increased quantity of entanglement from the vacuum in the presence of curvature [26]. Also, the Unruh-DeWitt detectors represent a tool to discover some space-time and entanglement harvesting properties, such as the effects of horizons on entanglement [27]; the degradation of the amount of entanglement in the presence of a reflecting boundary [28]; new information protocols in Schwarzschild black hole space-time [29]; and more recently the effects of field temperature on entanglement harvesting [30]. Moreover, these developments not only help the understanding of the vacuum structure, but they also explain the consequences and the implications of the vacuum structure in other areas of physics, such as cosmology, astrophysics, particle physics, among others. For instance, Henderson [31] implemented a two Unruh-DeWitt detectors protocol in the vicinity of a black hole which revealed that black holes inhibit entanglement harvesting .

Besides, there have been several articles surrounding the idea of multipartite entanglement. For example, there have been some developments on bipartite, tripartite, and tetrapartite entanglement in non-inertial frames, [32–34] and in inertial frames [10]. Also, the idea of multipartite entanglement has been highly explored for pure states [10, 20].

In particular, tripartite states are more difficult to compute and so there are not as many useful results as for bipartite states. Nevertheless, to assess entanglement in tripartite states the

Three-tangle and the π-tangle, or the Three-π, are two important entanglement measures [7]. On the one hand, the Three-tangle uses the concurrence. On the other hand, the π-tangle relies on negativity. Both, concurrence and negativity are also important entanglement measures that are very useful in bipartite states [35]. Furthermore, the existence of these two measurements for tripartite systems bring the possibility to analyze different types of states easier.

However, as previously mentioned, there is very little in the literature about extracting multipartite entanglement from the quantum vacuum. Now the purpose of this research is to evaluate the possibility of extracting tripartite entanglement from a quantum field, and its dependency on the detector's separation and their energy gap. Furthermore, another point to asses is the advantage and practicability of the use of π-tangle as an entanglement measurement.

2.2 Justification

Previous work has been done to quantify the entanglement of a multipartite state alone or in an accelerated frame. However, the multipartite structure of the vacuum has not been studied, specifically its tripartite entanglement. Over the last ten years, Unruh-DeWitt detectors have been used to extract bipartite entanglement from a quantum vacuum, and all the research has been done with only two uncorrelated detectors.

The purpose of this project is to employ three detectors to study tripartite entanglement of the quantum vacuum. Three detectors can give more information about the vacuum structure, possibly opening a new area of research as three detectors have more possibilities of arrangement. For example, if we want one detector near the even horizon, one across the event horizon and one falling in.

Even though there are multiple ways to measure entanglement, not all of them work for all types of states. So the reason π-tangle is used in the present work is because the final state is not pure or in a known form, such as W or Greenberger-Horne-Zeilinger (GHZ) classes, so we need an entanglement measure compatible with a state in a general form for a tripartite mixed system, which happens to be the π-tangle.

The entanglement harvesting implies the extraction of entanglement without measuring it directly. In addition, this work constitutes one step further towards the answer of the general question: how much multipartite entanglement can we harvest from the quantum vacuum?

2.3 Objectives

- To implement a general density matrix formation for a tripartite system of Unruh-DeWitt detectors once they have interacted with a quantum field. The approach shall utilize an unitary time evolution operator with the purpose to be used for entanglement harvesting via the π-tangle.

- Evaluate the difference in the quantity of entanglement between a triangle and linear Unruh-DeWitt detectors arrangements through the comparison of the resulting π-tangle values by studying the influence of the positioning of various detectors.

- Assess if π-tangle is a correct way to quantify entanglement of a tripartite mixed state. The latter by evaluating it with the constructed density matrix to verify its veracity in this kind of systems.

- Evaluate Perturbation Theory in a multipartite system to evaluate the results of π-tangle and consider the use of different switching functions.

- Harvest multipartite entanglement from a quantum vacuum through three Unruh-DeWitt detectors using the π-tangle. This in order to quantify the entanglement of two possible detector arrangements in a flat Minkowski space-time to take one step further to understand the quantum vacuum, and contribute to the development of quantum technology.

Chapter 3

Theoretical Basis

We present the basic concepts and definitions that will be the building blocks of the thesis project. Starting from the very basis of quantum mechanics, a brief historical background that ended with a change of paradigm and built new concepts here presented. The main concepts and definitions we are going to need are the density matrix, the partial trace, the partial transpose. Then we will dive into the concept of entanglement and the process of measure it through the negativity and, specifically for the present work, the π-tangle. Next, we need the very basic notion of quantum field theory and the definition of the simplest field: the scalar field. Finally, we will take into consideration the Wightman function, which is an important, but not very explicit, step in the process of calculating the π-tangle.

3.1 Quantum Mechanics

At the end of the 19th century, some of the performed experiments disagreed with the predictions of classical mechanics. The new discoveries led to a change of paradigm in the science made until that moment, changing our understanding of Nature. A new theory, quantum mechanics, emerged to describe the phenomena of the microscopic world that agree with the observed events. In the next sections some of the definitions of quantum mechanics will be exposed.

3.1.1 Density Matrix

The density matrix or density operator is an alternate representation of a quantum state [36]. In practice, the state vector $|\psi\rangle$ is not determined perfectly. That leads to the problem of the absence of the system's information. Then the question is how to take the partial information and to include it into the description of the laws of probability theory, both classical and quantum [11]. Here is where the density matrix enters.

We define the density operator as

$$\rho \equiv \sum_k p_k \left|\psi_k\right\rangle \left\langle\psi_k\right| \tag{3.1.1.1}$$

where p_k is the probability of each state and, given the vector representation of the state with an orthonormal basis $|i\rangle$, it is natural to associate the density operator with a matrix which elements are

$$\rho_{ij} \equiv \left\langle i\right| \rho \left|j\right\rangle \tag{3.1.1.2}$$

Besides, the density operator has to satisfy the following properties [11]:

1) ρ is Hermitian. This means that $\rho_{ij}^* = \rho_{ij}$.

2) ρ has unit trace:

$$Tr(\rho) = \sum_k p_k = 1 \tag{3.1.1.3}$$

3) ρ is a non-negative operator; that is, for any vector $|\phi\rangle$ in the Hilbert space $\mathcal{H}$ we have $\langle\phi| \rho |\phi\rangle \geq 0$

3.1.2 Partial trace

The partial trace Tr_B is a mapping from the density matrix ρ_{AB} on a composite space $\mathcal{H}_A \otimes \mathcal{H}_B$ onto density matrices ρ_A on $\mathcal{H}_A$. Let $|a_i\rangle$ be a basis of $\mathcal{H}_A$, and $|b_i\rangle$ be a basis of $\mathcal{H}_B$. Any density matrix ρ_{AB} on $\mathcal{H}_A \otimes \mathcal{H}_B$ can then be decomposed as

$$\rho_{AB} = c_{ijkl} \left|a_i\right\rangle \left\langle a_j\right| \otimes \left|b_k\right\rangle \left\langle b_l\right|$$

and the partial trace reads

$$Tr_B(\rho_{AB}) = c_{ijkl} \left|a_i\right\rangle \left\langle a_j\right| \left\langle b_l|b_k\right\rangle$$

which is a density matrix ρ_A on $\mathcal{H}_A$ [37].

3.1.3 Partial transpose

By definition, the transposition map $\mathcal{T}$ is linear and acts on the computational basis as:

$$\mathcal{T}(\sum_{j,k} c_{jk}) \left|j\right\rangle \left\langle k\right| := \sum_{j,k} c_{jk} \mathcal{T}(\left|j\right\rangle \left\langle k\right|) := \sum_{j,k} c_{jk} \left|k\right\rangle \left\langle j\right| \tag{3.1.3.1}$$

where $|j\rangle$ is the computational basis and c_{jk} are the matrix elements.

In comparison, the partial transpose is also linear but it takes the transpose over a subsystem, leaving the second one identical.

For multipartite systems, let's consider a density operator ρ in the Hilbert space $\mathcal{H} = \mathcal{H}_A \otimes \mathcal{H}_B \otimes \mathcal{H}_C \otimes ...$

$$\rho = \sum_{j_a,k_a}^{d_a} \sum_{j_b,k_b}^{d_b} \sum_{j_c,k_c}^{d_c} ... \left\langle j_a, j_b, j_c, ...\right| \rho \left|k_a, k_b, k_c, ...\right\rangle \left|j_a, j_b, j_c, ...\right\rangle \left\langle k_a, k_b, k_c, ...\right|$$

Where $|j\rangle$ and $|k\rangle$ are again the computational basis, $\langle j_a, j_b, j_c, ...| \rho |k_a, k_b, k_c, ...\rangle$ are the matrix elements and $d_a, d_b, d_c, ...$ are the dimensions of $\mathcal{H}_a, \mathcal{H}_b, \mathcal{H}_c, ...$, respectively. Then, the partial transpose over the subsystem a is defined as

$$\begin{aligned}
\mathcal{T}_a(\rho) &\equiv \mathcal{T} \otimes id_b(\rho) \otimes id_c(\rho) \otimes ... \\
&= \sum_{j_a,k_a}^{d_a} \sum_{j_b,k_b}^{d_b} \sum_{j_c,k_c}^{d_c} ... \left\langle j_a, j_b, j_c, ...\right| \rho \left|k_a, k_b, k_c, ...\right\rangle \mathcal{T}(\left|j_a\right\rangle \left\langle k_a,\right|) \otimes id(\left|j_b\right\rangle \left\langle k_b\right|) \otimes id(\left|j_c\right\rangle \left\langle k_c\right|) \otimes ... \\
&= \sum_{j_a,k_a}^{d_a} \sum_{j_b,k_b}^{d_b} \sum_{j_c,k_c}^{d_c} ... \left\langle j_a, j_b, j_c, ...\right| \rho \left|k_a, k_b, k_c, ...\right\rangle \left|k_a\right\rangle \left\langle j_a,\right| \otimes \left|j_b\right\rangle \left\langle k_b\right| \otimes \left|j_c\right\rangle \left\langle k_c\right| \otimes ... \\
&= \sum_{j_a,k_a}^{d_a} \sum_{j_b,k_b}^{d_b} \sum_{j_c,k_c}^{d_c} ... \left\langle j_a, j_b, j_c, ...\right| \rho \left|k_a, k_b, k_c, ...\right\rangle \left|k_a, j_b, j_c, ...\right\rangle \left\langle j_a, k_b, k_c, ...\right|
\end{aligned}$$

Similarly for the subsystem b

$$\begin{aligned}\mathcal{T}_b(\rho) &\equiv id_a(\rho)\otimes\mathcal{T}\otimes id_c(\rho)\otimes ...\\ &=\sum_{j_a,k_a}^{d_a}\sum_{j_b,k_b}^{d_b}\sum_{j_c,k_c}^{d_c}...\langle j_a,j_b,j_c,...|\,\rho\,|k_a,k_b,k_c,...\rangle\, id(|j_a\rangle\langle k_a,|)\otimes\mathcal{T}(|j_b\rangle\langle k_b|)\otimes id(|j_c\rangle\langle k_c|)\otimes ...\\ &=\sum_{j_a,k_a}^{d_a}\sum_{j_b,k_b}^{d_b}\sum_{j_c,k_c}^{d_c}...\langle j_a,j_b,j_c,...|\,\rho\,|k_a,k_b,k_c,...\rangle\,|j_a\rangle\langle k_a,|\otimes|k_b\rangle\langle j_b|\otimes|j_c\rangle\langle k_c|\otimes ...\\ &=\sum_{j_a,k_a}^{d_a}\sum_{j_b,k_b}^{d_b}\sum_{j_c,k_c}^{d_c}...\langle j_a,j_b,j_c,...|\,\rho\,|k_a,k_b,k_c,...\rangle\,|j_a,k_b,j_c,...\rangle\langle k_a,j_b,k_c,...|\end{aligned}$$

and analogously for all the subsystems.

The importance of the partial transpose relies mainly on the entanglement testing and quantification[38].

3.1.4 Entanglement

The concept of entanglement arises from the quantum theory to identify quantum correlations that happens in a quantum state from the ones in a classical state. Recent theories on quantum information developed a rigorous way to define such correlations. This relies on the concept of *local operations* possibly supplemented by *classical communication* (LOCC operations). "*LOCC*" concept can be broken down in two sections. First, the local operations are unitary transformations or measurements performed by one of the states on their members of the shared quantum state. Second, classical communications enables the entire state to share the results, in order to select the maximally entangled case. Then, the classical correlations are the ones that have been made through LOCC. If the correlation can not be simulated classically or it has not been created by LOCC alone, then it is associated to quantum effects. This last definition is an operative definition of entanglement. Given that definition, Beneti, *et al.* (2019) established in his book that it is possible to set forth some general statements[11]:

1. A separable state contains no entanglement. The concept of separability can be defined through a state generated through LOCC only: Let's begin with the multipartite state

$$\rho_{ABC...}=\sum_k p_k\rho_A^{(k)}\otimes\rho_B^{(k)}\otimes\rho_C^{(k)}\otimes ... \tag{3.1.4.1}$$

Then, the party A samples from the probability distribution $p_1, p_2, ...$, informs all other parties of the k-th outcome, and then each party X locally creates $\rho_X^{(k)}$. This implies that all the correlations in equation 3.1.4.1 can be described classically, therefore the state is not entangled.

2. No separable states are entangled. As separable states have to be created through LOCC and contain no entanglement, then it is clear that quantum states that cannot be generated through LOCC alone if and only if they are entangled. In addition, it is possible to say that *non-separable* and *entangled* are synonymous.

3. Entanglement cannot increase under LOCC. Any two states that are related by local unitaries must have an equal amount of entanglement. This means that if we have a state ρ and we transform it through LOCC to another state σ, then anything doable with σ and LOCC can also be achieved with ρ and LOCC.

3.1.5 Negativity

Quantification of entanglement relies in one basic question: "*Given a generic quantum state, pure or mixed, is it separable or entangled?*"[11].

On the one hand, in the bipartite case there are a lot of criteria to measure entanglement such as the positive partial transpose criterion; separability via positive, but not completely positive, maps; separability via entanglement witnesses Entanglement; matrix realignment criterion and linear contraction criteria, among others[20].

On the other hand, in multipartite states separability is not trivial as the systems become more complicated and this criterion is not necessarily an indicator of multipartite entanglement. For example, there can be a tripartite state that has bipartite entanglement but subsystem is uncorrelated with the other two. With the previous idea, it is very difficult to find an unambiguous definition of entanglement measures[11]. Most of the multipartite entanglement measures exist only for pure states as there is not a lot of research on mixed states because of their complexity.

A basic property of any resource criterion is that its value cannot be increased using free operations. This is called monotonicity [39]. One of the LOCC monotones is the *Negativity*[40], which is a simple computable measure of entanglement [20]. It is defined as

$$\mathcal{N}(\rho) = \sum_{\lambda<0} |\lambda| \tag{3.1.5.1}$$

where λ are the eigenvalues of the matrix ρ.

3.1.6 π-tangle

The π-tangle is a measure of entanglement for tripartite systems, that, compared to the three-tangle, works either for pure or mixed states. It uses the negativity, another strong way to quantify entanglement. π-tangle is derived from the Coffman-Kundu-Wootters inequality (CWK) in equation 3.1.6.1, and using the fact that the negativity is always equal or less than the concurrence ($\mathcal{N} \leq \mathcal{C}$) for each subsystem we can turn the CWK-inequality into equation 3.1.6.2.

$$\mathcal{C}^2_{A(B)} + \mathcal{C}^2_{A(C)} \leq \mathcal{C}^2_{A(BC)} \tag{3.1.6.1}$$

$$\mathcal{N}^2_{A(B)} + \mathcal{N}^2_{A(C)} \leq \mathcal{N}^2_{A(BC)} \tag{3.1.6.2}$$

Then the π-tangle can be interpreted as a residual entanglement when it is defined as

$$\pi_A = \mathcal{N}^2_{A(BC)} - \mathcal{N}^2_{A(B)} - \mathcal{N}^2_{A(C)} \tag{3.1.6.3}$$

and similarly for subsystems B and C.

Both, concurrence and negativity, are entanglement monotones, which means that they increase as entanglement increases. By contrast, the π-tangle has not been proven to be an entanglement monotone. However as it uses the negativity of the whole system and the subsystems, we can trust its results. Besides, we need an entanglement measure compatible with a state in a general form for a tripartite mixed system, which happens to be the π-tangle defined as

$$\pi = \frac{\pi_A + \pi_B + \pi_C}{3} \tag{3.1.6.4}$$

The purpose of π-tangle as an entanglement measurement to quantify three-qubit entanglement in terms of negativity was established by Ou and Fan in 2007 [41].

3.2 Quantum Field Theory

Quantum Field Theory (QFT) was born as a consequence of the efforts for the unification of quantum mechanics and special relativity. It was with this confluence that a new set of phenomena arises: Particles can be born and particles can die. That discovery required the development of a new subject in physics: quantum field theory.

The main idea of QFT is to treat particles as excitations of a field. The notion is that *"every particle and every wave in the Universe is simply an excitation of a quantum field that is defined over all space and time"* [42].

Classically we understand a field by a set of equations that govern the behavior of certain phenomena such as gravity or electromagnetism. We think that the field oscillates in space and time (at least for electromagnetic fields) and that is why we can find wave-like excitations from that field.

On the other hand, non-relativistic quantum mechanics treats particles as an entity described by the Schrödinger equation as a wave function, but regardless of the mathematical description, the particle will remain the same particle forever. However, special relativity establishes that matter can be transformed into energy and vice-versa. Then, if an electron is energetic enough, an electron and an "anti-electron" (or positron) can be produced. This phenomenon can not be described by the Schrödinger equation.

In this thesis we shall consider massless, scalar bosonic fields on 3+1 dimensional Minkowski spacetimes for simplicity. Here I present a short introduction starting with the action and equations of motion, discussing field expansions and commutation relations, and culminating in a short calculation of the Wightman function in 3+1 dimensions. This review relies on various sources [42–45]

3.2.1 Scalar field

The simplest Lagrangian is the one for a massless scalar field $\phi(x)$. By definition, a scalar field assigns a scalar amplitude to each position x in spacetime. The Lagrangian will depend in the gradient $\partial_\mu\phi \equiv \partial\phi/\partial x^\mu$ where x^μ (μ = 1,2,3) are the space coordinates and x^0 is the time coordinate. Then we define the Lagrangian ($\mathcal{L}$) to be:

$$\mathcal{L}_0 = \frac{1}{2}\partial_\mu\phi\partial^\mu\phi = \frac{1}{2}(\partial_\mu\phi)^2 \tag{3.2.1.1}$$

that can be expanded as:

$$\mathcal{L} = \frac{1}{2}(\partial_0\phi)^2 - \frac{1}{2}\nabla\phi\cdot\nabla\phi \tag{3.2.1.2}$$

which has the structure of $\mathcal{L}$ = kinetic energy − potential energy.

With the Lagrangian in equation 3.2.1.1 we have

$$\frac{\partial\mathcal{L}}{\partial\phi} = 0, \quad \frac{\partial\mathcal{L}}{\partial(\partial_\mu\phi)} = \partial^\mu\phi \tag{3.2.1.3}$$

and plugging the Euler-Lagrange equation defined as

$$\frac{\partial\mathcal{L}}{\partial\phi} - \partial_\mu\left(\frac{\partial\mathcal{L}}{\partial(\partial_\mu\phi)}\right) = 0 \tag{3.2.1.4}$$

we have

$$\partial_\mu\partial^\mu\phi = 0 \tag{3.2.1.5}$$

which is better known to have the form of a wave equation $\partial^2\phi = 0$ or $\frac{\partial^2\phi}{\partial t^2} - \nabla^2\phi = 0$, and has wave-like solutions in natural units ($c = 1$ and $\hbar = 1$)

$$u_{\boldsymbol{k}} = e^{-i(|\boldsymbol{k}|t - \boldsymbol{x}\cdot\boldsymbol{k})} \quad \text{and} \quad u^*_{\boldsymbol{k}} = e^{i(|\boldsymbol{k}|t - \boldsymbol{x}\cdot\boldsymbol{k})} \tag{3.2.1.6}$$

Now we can express a classical scalar field as

$$\phi(\boldsymbol{x}, t) = \int d^n\boldsymbol{k}(a^*_{\boldsymbol{k}}u^*_{\boldsymbol{k}} + a_{\boldsymbol{k}}u_{\boldsymbol{k}}) \tag{3.2.1.7}$$

where a and a^* are complex amplitudes that will depend on dimension (n) and $|\boldsymbol{k}|$.

Moreover, to quantize the field, we impose the canonical commutation relations on the field and its canonical conjugate momentum $\hat{\pi} = \partial_t\hat{\phi}$, promoting them both to operator status:

$$[\hat{\phi}(\boldsymbol{x}), \hat{\pi}(\boldsymbol{y})] = i\delta^n(\boldsymbol{x} - \boldsymbol{y}); \quad [\hat{\phi}(\boldsymbol{x}), \phi(\boldsymbol{y})] = [\hat{\pi}(\boldsymbol{x}), \pi(\boldsymbol{y})] = 0 \tag{3.2.1.8}$$

With these conditions, the complex amplitudes a and a^* become the creation or annihilation operators $\hat{a}_{\boldsymbol{k}}$ and $\hat{a}^\dagger_{\boldsymbol{k}}$ respectively. These operators have their canonical commutation relations

$$[\hat{a}_{\boldsymbol{k}}, \hat{a}^\dagger_{\boldsymbol{k}}] = \delta^n(\boldsymbol{k} - \boldsymbol{k'}); \quad [\hat{a}_{\boldsymbol{k}}, \hat{a}_{\boldsymbol{k}}] = [\hat{a}^\dagger_{\boldsymbol{k}}, \hat{a}^\dagger_{\boldsymbol{k}}] = 0 \tag{3.2.1.9}$$

Therefore, we can write the full field operator as

$$\hat{\phi}(\boldsymbol{x}, t) = \int \frac{d^n\boldsymbol{k}}{\sqrt{2(2\pi)^n|\boldsymbol{k}|}}(\hat{a}^\dagger_{\boldsymbol{k}} u^*_{\boldsymbol{k}} + \hat{a}_{\boldsymbol{k}} u_{\boldsymbol{k}}) \tag{3.2.1.10}$$

where the normalization factor $\frac{1}{\sqrt{2(2\pi)^n|\boldsymbol{k}|}}$ came from the normalization and the commutation relation for the annihilation and creation operators.

3.2.2 Wightman Function for a 3+1 Minkowski space

Around 1950, physicist Arthur Wightman wanted to give quantum field theory the mathematical formalism similar to the one developed by von Neuman for quantum mechanics [46]. Wightman then formulated the now well-known Wightman axioms, which were published only in 1964 because no nontrivial examples existed at that time [47].

In this axiomatic approach from Wightman, the basic field operators are usually realized as operator-valued distributions. Then, the operator-valued distributions satisfying the Wightman Axioms are called the Wightman fields. Finally, the Wightman functions are the correlation functions of Wightman fields [48]. The importance of the Wightman function in the present work is that the Wightman function also determines the response of particle detectors in a given state of motion [49].

We will now derive the Wightman function for a in a 3+1 dimensional flat spacetime. Let $|0\rangle$ denote the Minkowski vacuum state and using the full field operator with $n = 3$, the Wightman

function may be computed as

$$\begin{aligned}
\mathcal{W}(x,x') :&= \langle 0|\, \phi(x)\phi(x')\, |0\rangle \\
&= \int \frac{dk^3}{2(2\pi)^3|\boldsymbol{k}|} e^{i\boldsymbol{k}\cdot(\boldsymbol{x}-\boldsymbol{x'})-i|\boldsymbol{k}|(t-t')} \\
&= \frac{1}{4\pi^2|\boldsymbol{x}-\boldsymbol{x'}|}\int_0^\infty d|\boldsymbol{k}| e^{-i|\boldsymbol{k}|(t-t')}\sin(|\boldsymbol{k}||\boldsymbol{x}-\boldsymbol{x'}|) \\
&= \frac{1}{4\pi^2|\boldsymbol{x}-\boldsymbol{x'}|}\lim_{\epsilon\to 0^+}\int_0^\infty e^{-i|\boldsymbol{k}|[(t-t')-i\epsilon\,\mathrm{sgn}(t-t')]}\sin(|\boldsymbol{k}||\boldsymbol{x}-\boldsymbol{x'}|) \\
&= -\frac{1}{4\pi^2}\lim_{\epsilon\to 0^+}\frac{1}{[t-t'-i\epsilon\,\mathrm{sgn}(t-t')]^2-\boldsymbol{x}^2} \\
&= \frac{1}{4\pi i}\,\mathrm{sgn}(t-t')\delta[\sigma(x,x')] - \frac{1}{4\pi^2\sigma(x,x')}
\end{aligned} \tag{3.2.2.1}$$

where

$$\sigma(x,x') := (t-t')^2-(x-x')^2-(y-y')^2-(z-z')^2 \tag{3.2.2.2}$$

3.2.3 Entanglement Harvesting

As stated before, the property of entanglement in quantum systems has been one of the most surprising derivations from quantum mechanics. Since then, it has been studied in several areas of physics from condensed matter to the explanation of black hole entropy. All these studies have been an approach from quantum field theory.

Within the framework of algebraic quantum field theory, Summers and Werner [18, 50, 51] demonstrated that the vacuum state of a free quantum field in Minkowski space, as seen by local inertial observers, is entangled, and that the correlations seen by these observers are strong enough to violate Bell-type inequalities, even if these observers are in spacelike separated regions. This result implies that the observation of the vacuum fluctuations is enough to detect a violation of Bell's inequality and a source of entanglement is not required.

Later, Valentini [16] suggested that the cause of the correlation of two initially uncorrelated atoms in an electromagnetic vacuum, was either non-local photon propagation or a consequence of non-locally-correlated vacuum fluctuations. Years later, Reznick [18] demonstrated a similar effect using two Unruh-DeWitt detectors interacting locally with the vacuum state of a scalar field.

It is this process of extracting entanglement or nonlocal correlations from the vacuum state of a quantum field through localized detectors which now has become the definition of Entanglement Harvesting. Since then, entanglement harvesting has been shown to be sensitive to the background geometry of spacetime[52], as well as the topology [53]. It has also been implementation proposals for entanglement harvesting, for example, Onoe *et al,*[19] proposed that the nonlinear interaction behind the electro-optic effect can be reformulated in terms of an Unruh-DeWitt detector coupled to a conjugate field during a very short time interval. Another example is the proposal of Sabín *et al.* [54], in which they come up with the idea of a realistic circuit quantum electrodynamics (QED) experiment to test the extraction of past-future vacuum entanglement to a pair of superconducting qubits.

The convenience to use Unruh-DeWitt detectors to study the entanglement structure of a quantum field is that, the approach is mainly operational, in other words, the measuring process is explicitly described and the observer's motion can easily be taken into account; and, the mathematical methods are simple compared to algebraic quantum field theory and other methods.

Chapter 4

Methodology

In this chapter is also included the Unruh-DeWitt detector model that will be expanded later into three detectors. It is also expose the mathematical developments to calculate the π-tangle through the negativity of the tripartite and bipartite systems.

An Unruh-DeWitt detector is a two-level energy particle with $|0\rangle_D$ and $|1\rangle_D$ corresponding to the ground and excited levels respectively of the D detector and will form an orthonormal basis in the Hilbert space. The energy gap between the two levels is Ω and for the purpose of this work this gap is going to be equal for the three detectors. The Hamiltonian for the free evolution of each detector is going to be

$$H_o = \sum_D \frac{\Omega}{2}(|1\rangle_D \langle 1|_D - |0\rangle_D \langle 0|_D) \tag{4.0.0.1}$$

As these particles will interact with a scalar field, we need an interaction Hamiltonian that behaves as an atom's interaction with an electromagnetic field with a function that will control the duration of the interaction between the atom and the field.

For a single particle in an electromagnetic field, the interaction Hamiltonian is defined as

$$H_{int} = -\frac{e}{m}\vec{A} \cdot \vec{p} \tag{4.0.0.2}$$

where e and m are the charge and the mass of the electron, $\vec{p}$ is the momentum and $\vec{A}$ is the vector potential[55].

However, to treat the interaction between an atomic electron and a field it is more convenient to use the so-called multipolar Hamiltonian where equation 4.0.0.2 takes the form

$$H_{int} = -e\vec{X} \cdot \vec{E}(\vec{x}, t) \tag{4.0.0.3}$$

where $\vec{E}$ is the electric field and as $e\vec{X}$ is the dipole moment of the charge e, equation 4.0.0.3 is known as the electric dipole form of the interaction [56].

In order to simplify the analysis of the problem, we now proceed to move to the interaction picture (or the Dirac Picture) of the Hamiltonian defined as

$$H_I := e^{iH_o t} H_{int} e^{-iH_o t} \tag{4.0.0.4}$$

If now we substitute equations 4.0.0.3 and 4.0.0.1 in 4.0.0.4 and we expand $\vec{X}$ as $\vec{X} = \int d\vec{x}\vec{x} \left|\vec{x}\right\rangle \left\langle\vec{x}\right|$ we can get

$$\begin{aligned} H_I &= e^{i\frac{\Omega}{2}t} \left|1\right\rangle_D \left\langle 0\right|_D \otimes \int d\vec{x} \left\langle 1|\vec{x}\right\rangle \vec{x} \left\langle\vec{x}|0\right\rangle \cdot \vec{E}(\vec{x}, t) + e^{-i\frac{\Omega}{2}t} \left|0\right\rangle_D \left\langle 1\right|_D \otimes \int d\vec{x} \left\langle 0|\vec{x}\right\rangle \vec{x} \left\langle\vec{x}|1\right\rangle \cdot \vec{E}(\vec{x}, t) \\ &= e^{i\Omega\tau} \left|1\right\rangle_D \left\langle 0\right|_D \otimes \int d\vec{x}\vec{F}(\vec{x}) \cdot \vec{E}(\vec{x}, t) + e^{-i\Omega\tau} \left|0\right\rangle_D \left\langle 1\right|_D \otimes \int d\vec{x}\vec{F}^*(\vec{x}) \cdot \vec{E}(\vec{x}, t) \end{aligned}$$

Assuming that the spatial extent of the atom is sufficiently localized so that the function $\vec{F}(\vec{x}) = \left\langle 1|\vec{x}\right\rangle \vec{x} \left\langle\vec{x}|0\right\rangle$ may be approximated as a delta function $\vec{F}(\vec{x}) \approx \delta^3(\vec{x} - \vec{x}_D(\tau))$ where $\vec{x}_D(\tau)$ is the trajectory of the atom parametrized in terms of its proper time τ.

Although the Unruh-DeWitt interaction Hamiltonian has a similar form as the electric dipole Hamiltonian, the correct description of the system requires some changes. First, the field that interacts with the detectors is a scalar field $\phi(x)$ instead of an electric field. Furthermore, a switching function $\chi_D \in [0, 1]$ is now introduced, which will control the duration of the interaction between the field and the detectors, and is defined as

$$\chi_D(\tau) = e^{-\tau^2/2\sigma^2} \tag{4.0.0.5}$$

Therefore, the interaction Hamiltonian can be written as

$$H_D(\tau) = \lambda\chi_D(\tau)(\sigma^+(\tau) + \sigma^-(\tau)) \otimes \phi[x_D(\tau)] \tag{4.0.0.6}$$

where $\lambda \ll 1$ is the interaction strength and

$$\sigma^+(\tau) := e^{i\Omega\tau} \left|1\right\rangle_D \left\langle 0\right|_D ; \sigma^-(\tau) := e^{-i\Omega\tau} \left|0\right\rangle_D \left\langle 1\right|_D$$

are the ladder operators. In this kind of approximation of a two-level atom with the electromagnetic field, the atom is referred to as an Unruh-DeWitt detector. The time evolution of the detector and field during the measuring process, is described by the unitary operator generated by the interaction Hamiltonian in 4.0.0.6, and Perturbation Theory is used to expand it in power series to make it easy to use and solve so the resulting unitary operator is

$$\begin{aligned} U &:= \mathcal{T}\exp\left\{-i\int d\tau H_D(\tau)\right\} \\ &= 1 + (-i\lambda)\int d\tau H_D(\tau) + \frac{(-i\lambda)^2}{2}\int d\tau d\tau' \mathcal{T} H_D(\tau)H_D(\tau') + \mathcal{O}(\lambda^3) \end{aligned} \tag{4.0.0.7}$$

where T defined as $TA(t)B(t') := \theta(t-t')A(t)B(t') + \theta(t'-t)B(t')A(t)$ is the time ordering operator. In addition, the integration interval of each integral is $\tau \in (-\infty, \infty)$.

If the detectors at the beginning ($\tau \to -\infty$) are prepared in the ground state $|0\rangle_D$ and the field in an appropriately defined vacuum state $|0\rangle$, then the final state after the measuring process will be

$$\begin{aligned} U|0\rangle_D|0\rangle &= \left(1 + (-i)\int d\tau H_D(\tau) + \frac{(-i)^2}{2}\int d\tau d\tau' \mathcal{T} H_D(\tau)H_D(\tau') + \mathcal{O}(\lambda^3)\right)|0\rangle_D|0\rangle \\ &= |0\rangle_D|0\rangle - i\lambda\int d\tau \chi_D(\tau)e^{i\Omega_D\tau}|1\rangle_D \otimes \phi[x_D(\tau)]|0\rangle \\ &- \frac{\lambda^2}{2}\int d\tau d\tau' \chi_D(\tau)\chi_D(\tau')\mathcal{T}[\sigma^-(\tau)\sigma^+(\tau') + \sigma^+(\tau)\sigma^-(\tau')]|0\rangle_D \\ &\otimes \mathcal{T}\phi[x_D(\tau)]\phi[x_D(\tau')]|0\rangle + \mathcal{O}(\lambda^3) \end{aligned} \tag{4.0.0.8}$$

The final state of the detectors is obtained by tracing over the field degrees of freedom with

$$\begin{aligned} \rho_{ABC} &:= tr_\phi(|\Psi_f\rangle\langle\Psi_f|) \\ &= \sum_{n,m}\lambda^{n+m}\int d\mu \langle\mu|(|\Psi_f\rangle\langle\Psi_f|)|\mu\rangle \end{aligned}$$

Also, the final state of each detector is also obtained by tracing over the other two detectors to get a final state

$$\rho_D = \begin{pmatrix} 1-P_D & 0 \\ 0 & P_D \end{pmatrix} + \mathcal{O}(\lambda^4)$$

where $P_D(\tau)$ is defined as

$$P_D(\tau) = \lambda^2 \int_{-\infty}^{\tau} dt \int_{-\infty}^{\tau} dt \chi_D(t)\chi_D(t')e^{-i\omega(t-t')}W(x_D(t), x_D(t')) \tag{4.0.0.9}$$

and $W(x, x')$ is the vacuum Wightman function

$$W(x, x') := \langle 0| \phi(x)\phi(x') |0\rangle \tag{4.0.0.10}$$

In this present work, there will be two types of detector configuration. The first arrangement is having the detectors equally spaced as an equilateral triangle. And the second one is with the detectors aligned in the form that the first detector with the second and the second with the third are equally spaced but the first with the third are not. These two systems are going to have different values of the density matrix elements and have to be calculated separately.

After obtaining the density matrix, the next step is to calculate the π-tangle. There are some methods to measure the entanglement of the tripartite system. However, as the final state is a mixed state and not a pure one, we have to use the π-tangle which is defined in [41] as

$$\pi = \frac{\pi_A + \pi_B + \pi_C}{3} \tag{4.0.0.11}$$

where

$$\pi_A = \mathcal{N}^2_{A(BC)} - \mathcal{N}^2_{A(B)} - \mathcal{N}^2_{A(C)} \tag{4.0.0.12}$$

and like wise for π_B and π_C

$$\pi_B = \mathcal{N}^2_{B(AC)} - \mathcal{N}^2_{B(A)} - \mathcal{N}^2_{B(C)} \tag{4.0.0.13}$$

$$\pi_C = \mathcal{N}^2_{C(AB)} - \mathcal{N}^2_{C(B)} - \mathcal{N}^2_{C(A)} \tag{4.0.0.14}$$

and $\mathcal{N}$ is the negativity of the system defined as

$$\mathcal{N}_\rho := 2 \sum_{\lambda_i<0} |\lambda_i| \tag{4.0.0.15}$$

and λ_i the eigenvalues of ρ. In addition, we have to compute the negativity of each subsystem ($\mathcal{N}_{A(BC)}$,$\mathcal{N}_{A(B)}$, and so on). Hence, the definition of the negativity can be written as

$$\mathcal{N}_{A(BC)} = ||\rho^{T_A}_{ABC}|| - 1 \tag{4.0.0.16}$$

and

$$\mathcal{N}_{A(B)} = ||(Tr_C[\rho_{ABC}])^{T_A}|| - 1 \tag{4.0.0.17}$$

where the partial transpose ρ^{T_D} over the detector D can be computed as

$$\begin{aligned}\rho_{ABC}^{T_A} &= \sum_{ijk,i'j'k'} \eta\eta^* \left|ijk\right\rangle \left\langle i'j'k'\right|)^{T_A} \\ &= \sum_{ijk,i'j'k'} \eta\eta^* \left|i'jk\right\rangle \left\langle ij'k'\right| \end{aligned} \tag{4.0.0.18}$$

for some states $|ijk\rangle$ and coefficients η that are non-negative and add up to one; and the partial trace Tr_C is computed as

$$Tr_C[\rho_{ABC}] = \left\langle 0\right|_C \rho_{ABC} \left|0\right\rangle_C + \left\langle 1\right|_C \rho_{ABC} \left|1\right\rangle_C \tag{4.0.0.19}$$

All the numerical calculations and the figures were made via Mathematica software [57].

Chapter 5

Results and discussions

In this chapter the results and discussions of the thesis project are presented. First, it will be established the specific procedure followed for the construction of the general density matrix for the tripartite state after extracting the field from the system. Then, the final density matrix with the specific values we will use for the purpose of this work. Second, the structure of the system through the comparison with previous work made by Smith [58] in entanglement harvesting with two Unruh-DeWitt detectors. Third, the results obtained for the triangle arrangement and the discussion of the particularities founded. Next, we analyse those particularities from different perspectives: from the point of view of the specific variables used and from the point of view of the behavior of Perturbation Theory in our particular system. After that, the results for the linear arrangement and the comparison with the triangle case are presented.

5.1 Construction of the density matrix

Consider three Unruh-DeWitt detectors labeled A, B and C described by their Hilbert spaces $\mathcal{H}_A, \mathcal{H}_B$ and $\mathcal{H}_C$ respectively and each will have their proper time τ_D that depends on an appropriate coordinate time t. In addition, these detectors couple to an scalar field ϕ. The Hamiltonian for the free evolution 4.0.0.1 of the three atoms is going to be

$$H_o = \frac{\Omega}{2}(|1\rangle_A \langle 1|_A - |0\rangle_A \langle 0|_A) + \frac{\Omega}{2}(|1\rangle_B \langle 1|_B - |0\rangle_B \langle 0|_B) + \frac{\Omega}{2}(|1\rangle_C \langle 1|_C - |0\rangle_C \langle 0|_C) \quad (5.1.0.1)$$

Then, the time evolution operator for the atom-field interaction generated by the interaction Hamiltonian 5.1.0.1 is described by the following unitary operator

$$U = T\exp\Big[-i\int dt\Big(\frac{d\tau_A}{dt}H_A[\tau_A(t)] + \frac{d\tau_B}{dt}H_B[\tau_B(t)] + \frac{d\tau_C}{dt}H_C[\tau_C(t)]\Big)\Big] \tag{5.1.0.2}$$

which has to be expanded through Perturbation Theory as it can not be solved analytically with the Gaussian switching function. After the expansion to the third term, the time evolution operator can be expressed as

$$\begin{aligned}
U =& T\exp\Big[-i\int dt\Big(\frac{d\tau_A}{dt}H_A[\tau_A(t)] + \frac{d\tau_B}{dt}H_B[\tau_B(t)] + \frac{d\tau_C}{dt}H_C[\tau_C(t)]\Big)\Big] \\
=& 1 - i\int dt\Big(\frac{d\tau_A}{dt}H_A[\tau_A(t)] + \frac{d\tau_B}{dt}H_B[\tau_B(t)] + \frac{d\tau_C}{dt}H_C[\tau_C(t)]\Big) \\
&- \frac{1}{2}\int dtdt'T[\frac{d\tau_A}{dt}\frac{d\tau_A}{dt'}H_A[\tau_A(t)]H_A[\tau_A(t')] \\
&+ \frac{d\tau_B}{dt}\frac{d\tau_B}{dt'}H_B[\tau_B(t)]H_B[\tau_B(t')] + \frac{d\tau_C}{dt}\frac{d\tau_C}{dt'}H_C[\tau_C(t)]H_C[\tau_C(t')] \\
&+ \frac{d\tau_A}{dt}\frac{d\tau_B}{dt'}H_A[\tau_A(t)]H_B[\tau_B(t')] + \frac{d\tau_A}{dt}\frac{d\tau_C}{dt'}H_A[\tau_A(t)]H_C[\tau_C(t')] \\
&+ \frac{d\tau_B}{dt}\frac{d\tau_A}{dt'}H_B[\tau_B(t)]H_A[\tau_A(t')] + \frac{d\tau_B}{dt}\frac{d\tau_C}{dt'}H_B[\tau_B(t)]H_C[\tau_C(t')] \\
&+ \frac{d\tau_C}{dt}\frac{d\tau_A}{dt'}H_C[\tau_C(t)]H_A[\tau_A(t')] + \frac{d\tau_C}{dt}\frac{d\tau_B}{dt'}H_C[\tau_C(t)]H_B[\tau_B(t')]] + \mathcal{O}(\lambda^3)
\end{aligned}$$

where $\mathcal{O}(\lambda^3)$ encompasses the rest of the terms that are of larger order.

We now prepare the initial state at $t \to -\infty$ where each detector is at its base state, the field is in the vacuum state and the final state $|\Psi_f\rangle \in \mathcal{H}_A \otimes \mathcal{H}_B \otimes \mathcal{H}_C \otimes \mathcal{H}_\phi$. This is

$$|\Psi_i\rangle = |0\rangle_A |0\rangle_B |0\rangle_C |0\rangle_\phi \tag{5.1.0.3}$$

If the detectors are prepared in the base state and the field is the vacuum state, then their final state after the measuring process is the joint state

$$\begin{aligned}
|\Psi_f\rangle &= U|\Psi_i\rangle \\
&= U|0\rangle_A |0\rangle_B |0\rangle_C |0\rangle_\phi \\
&= \sum_n \lambda^n \left|\Psi^{(n)}\right\rangle
\end{aligned}$$

where $\left|\Psi^{(n)}\right\rangle$ is the n^{th} order contribution to $|\Psi_f\rangle$. Here we defined $\eta_D(t) := \chi_D(\tau_D(t))\frac{d\tau_D}{dt}$ and $\phi_D(t) := \phi[x_D(t)]$, where $x_D(t)$ are the trajectories followed by the detectors. The final state is then defined as

$$\left|\Psi^{(0)}\right\rangle = |0\rangle_A |0\rangle_B |0\rangle_C |0\rangle_\phi$$

$$\begin{aligned}\left|\Psi^{(1)}\right\rangle = -i \int dt(&\eta_A(t)e^{i\Omega_A\tau_A(t)} |1\rangle_A |0\rangle_B |0\rangle_C \otimes \phi_A(t) |0\rangle_\phi \\ &+ \eta_B(t)e^{i\Omega_B\tau_B(t)} |0\rangle_A |1\rangle_B |0\rangle_C \otimes \phi_B(t) |0\rangle_\phi \\ &+ \eta_C(t)e^{i\Omega_C\tau_C(t)} |0\rangle_A |0\rangle_B |1\rangle_C \otimes \phi_C(t) |0\rangle_\phi)\end{aligned}$$

$$\begin{aligned}\left|\Psi^{(2)}\right\rangle = -\frac{1}{2} \int dtdt'T[&\\ &\eta_A(t)\eta_A(t')[\sigma_A^+(t)\sigma_A^-(t) + \sigma_A^-(t)\sigma_A^+(t)] |0\rangle_A |0\rangle_B |0\rangle_C \otimes \phi_A(t)\phi_A(t')) |0\rangle_\phi \\ &+ \eta_B(t)\eta_B(t')[\sigma_B^+(t)\sigma_B^-(t) + \sigma_B^-(t)\sigma_B^+(t)] |0\rangle_A |0\rangle_B |0\rangle_C \otimes \phi_B(t)\phi_B(t')) |0\rangle_\phi \\ &+ \eta_C(t)\eta_C(t')[\sigma_C^+(t)\sigma_C^-(t) + \sigma_C^-(t)\sigma_C^+(t)] |0\rangle_A |0\rangle_B |0\rangle_C \otimes \phi_C(t)\phi_C(t')) |0\rangle_\phi \\ &+ (\eta_A(t)\eta_B(t')e^{i(\Omega_A\tau_A+\Omega_B\tau_B)} |1\rangle_A |1\rangle_B |0\rangle_C \otimes [\phi_A(t)\phi_B(t') + \phi_B(t)\phi_A(t')] |0\rangle_\phi) \\ &+ (\eta_A(t)\eta_C(t')e^{i(\Omega_A\tau_A+\Omega_C\tau_C)} |1\rangle_A |1\rangle_C |0\rangle_B \otimes [\phi_A(t)\phi_C(t') + \phi_C(t)\phi_A(t')] |0\rangle_\phi) \\ &+ (\eta_B(t)\eta_C(t')e^{i(\Omega_B\tau_B+\Omega_C\tau_C)} |1\rangle_B |1\rangle_C |0\rangle_A \otimes [\phi_B(t)\phi_C(t') + \phi_C(t)\phi_B(t')] |0\rangle_\phi)]\end{aligned}$$

$$
\begin{aligned}
\left|\Psi^{(3)}\right\rangle = \frac{i}{6}\int dtdt'dt''T[\\
&\eta_A(t)\eta_A(t')\eta_A(t'')(\sigma_A^-(t)\sigma_A^+(t)\sigma_A^-(t)+\sigma_A^+(t)\sigma_A^-(t)\sigma_A^+(t))\left|0\right\rangle_A\left|0\right\rangle_B\left|0\right\rangle_C\\
&\otimes\phi_A(t)\phi_A(t')\phi_A(t''))\left|0\right\rangle\\
&+\eta_B(t)\eta_B(t')\eta_B(t'')(\sigma_B^-(t)\sigma_B^+(t)\sigma_B^-(t)+\sigma_B^+(t)\sigma_B^-(t)\sigma_B^+(t))\left|0\right\rangle_A\left|0\right\rangle_B\left|0\right\rangle_C\\
&\otimes\phi_B(t)\phi_B(t')\phi_B(t''))\left|0\right\rangle\\
&+\eta_C(t)\eta_C(t')\eta_C(t'')(\sigma_C^-(t)\sigma_C^+(t)\sigma_C^-(t)+\sigma_C^+(t)\sigma_C^-(t)\sigma_C^+(t))\left|0\right\rangle_A\left|0\right\rangle_B\left|0\right\rangle_C\\
&\otimes\phi_C(t)\phi_C(t')\phi_C(t''))\left|0\right\rangle\\
&+(\eta_A(t)\eta_A(t')\eta_B(t'')e^{i(\Omega_A\tau_A+\Omega_A\tau_A+\Omega_B\tau_B)}\left|0\right\rangle_A\left|1\right\rangle_B\left|0\right\rangle_C\\
&\otimes[\phi_A(t)\phi_A(t')\phi_B(t'')+\phi_A(t)\phi_B(t')\phi_A(t'')+\phi_B(t)\phi_A(t')\phi_A(t'')]\left|0\right\rangle)\\
&+(\eta_A(t)\eta_A(t')\eta_C(t'')e^{i(\Omega_A\tau_A+\Omega_A\tau_A+\Omega_C\tau_C)}\left|0\right\rangle_A\left|0\right\rangle_B\left|1\right\rangle_C\\
&\otimes[\phi_A(t)\phi_A(t')\phi_C(t'')+\phi_A(t)\phi_C(t')\phi_A(t'')+\phi_C(t)\phi_A(t')\phi_A(t'')]\left|0\right\rangle)\\
&+(\eta_A(t)\eta_B(t')\eta_B(t'')e^{i(\Omega_A\tau_A+\Omega_B\tau_B+\Omega_B\tau_B)}\left|1\right\rangle_A\left|0\right\rangle_B\left|0\right\rangle_C\\
&\otimes[\phi_A(t)\phi_B(t')\phi_B(t'')+\phi_B(t)\phi_A(t')\phi_B(t'')+\phi_B(t)\phi_B(t')\phi_A(t'')]\left|0\right\rangle)\\
&+(\eta_A(t)\eta_C(t')\eta_C(t'')e^{i(\Omega_A\tau_A+\Omega_C\tau_C+\Omega_C\tau_C)}\left|1\right\rangle_A\left|0\right\rangle_B\left|0\right\rangle_C\\
&\otimes[\phi_A(t)\phi_C(t')\phi_C(t'')+\phi_C(t)\phi_A(t')\phi_C(t'')+\phi_C(t)\phi_C(t')\phi_A(t'')]\left|0\right\rangle)\\
&+(\eta_B(t)\eta_B(t')\eta_C(t'')e^{i(\Omega_B\tau_B+\Omega_B\tau_B+\Omega_C\tau_C)}\left|0\right\rangle_A\left|0\right\rangle_B\left|1\right\rangle_C\\
&\otimes[\phi_B(t)\phi_B(t')\phi_C(t'')+\phi_B(t)\phi_C(t')\phi_B(t'')+\phi_C(t)\phi_B(t')\phi_B(t'')]\left|0\right\rangle)\\
&+(\eta_B(t)\eta_C(t')\eta_C(t'')e^{i(\Omega_B\tau_B+\Omega_C\tau_C+\Omega_C\tau_C)}\left|0\right\rangle_A\left|1\right\rangle_B\left|0\right\rangle_C\\
&\otimes[\phi_B(t)\phi_C(t')\phi_C(t'')+\phi_C(t)\phi_C(t')\phi_B(t'')+\phi_C(t)\phi_B(t')\phi_C(t'')]\left|0\right\rangle)]\\
&+(\eta_A(t)\eta_B(t')\eta_C(t'')e^{i(\Omega_A\tau_A+\Omega_B\tau_B+\Omega_C\tau_C)}\left|1\right\rangle_A\left|1\right\rangle_B\left|1\right\rangle_C\\
&\otimes[\phi_A(t)\phi_B(t')\phi_C(t'')+\phi_A(t)\phi_C(t')\phi_B(t'')+\phi_B(t)\phi_A(t')\phi_C(t'')\\
&+\phi_B(t)\phi_C(t')\phi_A(t'')+\phi_C(t)\phi_A(t')\phi_B(t'')+\phi_C(t)\phi_B(t')\phi_A(t'')]\left|0\right\rangle)
\end{aligned}
$$

In order to evaluate only the final state of the detectors it is necessarily to trace over the field from the final state $|\Psi_f\rangle$ as

$$\rho_{ABC} := tr_\phi(|\Psi_f\rangle\langle\Psi_f|) \tag{5.1.0.4}$$

$$= \sum_{n,m}\lambda^{n+m}\int d\mu\,\langle\mu|\,(|\Psi_f\rangle\langle\Psi_f|)\,|\mu\rangle \tag{5.1.0.5}$$

It should be noted that field states that have an even number of excitations (*e.g* $|001\rangle$ or $|111\rangle$) are orthogonal to field states with an odd number of excitations (*e.g* $|011\rangle$ or $|000\rangle$), as they have an even and odd number of fields operators applied to the field vacuum, respectively. Thus, the terms that are going to survive at the moment of trace out the field are going to be the ones with both even (*e.g* $|001\rangle\langle 100|$) or odd number of excitations (*e.g* $|101\rangle\langle 110|$). Subsequently, there will be only parameters of 1-to-1, 1-to-3 0-to-2 and 2-to-2, and so on, interactions in the density matrix and zero everywhere else, where the terms are orthogonal.

Although the expansion of the time evolution operator is only to the third term, the general density matrix for a tripartite system should be constructed with all the terms in the expansion, independently of the specific parameters of the matrix.

Nevertheless, no matter how far the operator is expanded, it will have the same elements as it is expanded only to the fourth term; this expansion is presented in appendix A. All these arguments combined and applying equation 5.1.0.4 are going to give the general form of the density matrix for three detectors coupled with an scalar field.

$$\rho_{ABC} = \begin{pmatrix} \rho_{11} & 0 & 0 & 0 & \rho_{15} & \rho_{16} & \rho_{17} & 0 \\ 0 & \rho_{22} & \rho_{23} & \rho_{24} & 0 & 0 & 0 & \rho_{28} \\ 0 & \rho_{23}^{*} & \rho_{33} & \rho_{34} & 0 & 0 & 0 & \rho_{38} \\ 0 & \rho_{24}^{*} & \rho_{34}^{*} & \rho_{44} & 0 & 0 & 0 & \rho_{48} \\ \rho_{15}^{*} & 0 & 0 & 0 & \rho_{55} & \rho_{56} & \rho_{57} & 0 \\ \rho_{16}^{*} & 0 & 0 & 0 & \rho_{56}^{*} & \rho_{66} & \rho_{67} & 0 \\ \rho_{17}^{*} & 0 & 0 & 0 & \rho_{57}^{*} & \rho_{67}^{*} & \rho_{77} & 0 \\ 0 & \rho_{28}^{*} & \rho_{38}^{*} & \rho_{48}^{*} & 0 & 0 & 0 & \rho_{88} \end{pmatrix} \tag{5.1.0.6}$$

After the computation of each matrix element, this gives us the density matrix

$$\rho_{ABC} = \begin{pmatrix} 1-P_A-P_B-P_C & 0 & 0 & 0 & X_{CB} & X_{CA} & X_{BA} & 0 \\ 0 & P_C & C_{BC} & C_{AC} & 0 & 0 & 0 & \rho_{28} \\ 0 & C^*_{BC} & P_B & C_{AB} & 0 & 0 & 0 & \rho_{38} \\ 0 & C^*_{AC} & C^*_{AB} & P_A & 0 & 0 & 0 & \rho_{48} \\ X^*_{CB} & 0 & 0 & 0 & \rho_{55} & \rho_{56} & \rho_{57} & 0 \\ X^*_{CA} & 0 & 0 & 0 & \rho^*_{56} & \rho_{66} & \rho_{67} & 0 \\ X^*_{BA} & 0 & 0 & 0 & \rho^*_{57} & \rho^*_{67} & \rho_{77} & 0 \\ 0 & \rho^*_{28} & \rho^*_{38} & \rho^*_{48} & 0 & 0 & 0 & \rho_{88} \end{pmatrix} \tag{5.1.0.7}$$

where

$$P_D(\tau) = \lambda^2 \int_{-\infty}^{\tau} dt \int_{-\infty}^{\tau} dt \chi_D(t)\chi_D(t') e^{-i\omega(t-t')} W(x_D(t), x_D(t'))$$

$$C_{kj} = \lambda^2 \int dt dt' \eta_k(t)\eta_j(t') e^{i(\Omega_k \tau_k(t) - \Omega_j \tau_j(t'))} W(x_j(t'), x_k(t))$$

$$X_{jk} = -\lambda^2 \int_{t>t'} dt dt' [\eta_j(t)\eta_k(t') e^{-i(\Omega_j \tau_j(t) + \Omega_k \tau_k(t'))} W(x_k(t'), x_j(t)) + \eta_k(t)\eta_j(t') e^{-i(\Omega_k \tau_k(t) + \Omega_j \tau_j(t'))} W(x_j(t'), x_k(t))]$$

with

$$k \in [B, A, A] \qquad and \qquad j \in [C, C, B]$$

and $W(x, x')$ the Wightman function defined as in equation 4.0.0.10

Using the results previously calculated by Alexander Smith [58]

$$P = \frac{\lambda^2}{4\pi} \left[e^{-\sigma^2\Omega^2} - \sqrt{\pi}\sigma\Omega erfc(\sigma\Omega) \right] + \mathcal{O}(\lambda^4) \tag{5.1.0.8}$$

$$X = i\frac{\lambda^2}{4\sqrt{\pi}} \frac{\sigma}{L} e^{-\sigma^2\Omega^2 - L^2/4\sigma^2} \left[1 + erf\left(i\frac{L}{2\sigma} \right) \right] \tag{5.1.0.9}$$

$$C = \frac{\lambda^2}{4\sqrt{\pi}} \frac{\sigma}{L} e^{-L^2/4\sigma^2} \left(\mathrm{Im}\left[e^{iL\Omega} erf\left(i\frac{L}{2\sigma} + \sigma\Omega \right) \right] - \sin \Omega L \right) \tag{5.1.0.10}$$

The rest of the terms are of λ^4 and λ^6 order, which are very difficult to calculate analytically but are crucial to have a density matrix without a determinant equal to zero. It should be noted that to have a complete description of the system we shall include all the terms. However, based on previous works of entanglement harvesting of two Unruh-DeWitt detectors in which the λ^4 term is ignored, we made the supposition that major order terms should not contribute either in the tripartite system. Thus, if we ignore those terms, our density matrix in equation 5.1.0.7 ends up like

$$\rho_{ABC} = \begin{pmatrix} 1-P_A-P_B-P_C & 0 & 0 & 0 & X_{CB} & X_{CA} & X_{BA} & 0 \\ 0 & P_C & C_{BC} & C_{AC} & 0 & 0 & 0 & 0 \\ 0 & C^*_{BC} & P_B & C_{AB} & 0 & 0 & 0 & 0 \\ 0 & C^*_{AC} & C^*_{AB} & P_A & 0 & 0 & 0 & 0 \\ X^*_{CB} & 0 & 0 & 0 & 0 & 0 & 0 & 0 \\ X^*_{CA} & 0 & 0 & 0 & 0 & 0 & 0 & 0 \\ X^*_{BA} & 0 & 0 & 0 & 0 & 0 & 0 & 0 \\ 0 & 0 & 0 & 0 & 0 & 0 & 0 & 0 \end{pmatrix} \tag{5.1.0.11}$$

Although the expansion of the time evolution operator was up to the third, to have the general density matrix without considering the specific expressions for each matrix element, we would need to have the entire expression for the unitary operator or all the terms of the expansion. However, we only need to expand up to the fourth term to have all the non-zero elements in the matrix.

Another observation from the system is that despite the fact that Silman and Reznik [59] had the same general matrix structure and reduced it to a W-state ($\frac{1}{\sqrt{3}}(|100\rangle + |010\rangle + |001\rangle)$), the particularities of our system does not allow the matrix to be reduced to that state. It neither can be reduced to a GHZ-state ($\frac{1}{\sqrt{2}}(|000\rangle + |111\rangle)$) or a modification of it which could make our system easier to solve. Then, our system can not be easily solved by numerous methods for those states and we have to continue working with the PPT criterion, the negativity and the π-tangle which can be calculated only with the density matrix.

It is important to have the general form of the density matrix and to be valid, its determinant

has to be non-zero. With the general form we can start to evaluate the eigenvalues and make suppositions about our system. With this kind of matrix, we can reduce it to the form of a bipartite system and have the exact same results of the previous research on entanglement harvesting of two Unruh-DeWitt detectors.

5.2 Tripartite verification through bipartite system

In order to check if this density matrix is correct and valid, we should be able to reduce it to the interaction of only two of the detectors and this result must match with previously reported results [58]. So, first we reduce our density matrix tracing out one of the detectors and we must obtain the general form of a bipartite density matrix. And if we trace out again another detector, then we should get only the probability of the last detector.

Then, let's start by tracing out the detector C as

$$\begin{aligned}\rho_{AB} &= Tr_C[\rho_{ABC}] \\ &= \langle 0|_C \, \rho_{ABC} \, |0\rangle_C + \langle 1|_C \, \rho_{ABC} \, |1\rangle_C\end{aligned}$$

which lead us to

$$\rho_{AB} = \begin{pmatrix} 1-P_A-P_B & 0 & 0 & X_{BA} \\ 0 & P_B & C_{AB} & 0 \\ 0 & C_{AB}^* & P_A & 0 \\ X_{BA}^* & 0 & 0 & 0 \end{pmatrix} \tag{5.2.0.1}$$

and if we trace out one of the detectors again we get

$$\begin{aligned}\rho_A &= Tr_B[\rho_{AB}] \\ &= \begin{pmatrix} 1-P_A & 0 \\ 0 & P_A \end{pmatrix}\end{aligned}$$

This last result realizes that the tripartite system obtained can effectively be reduced to the bipartite system. From these data we can also replicate the results obtained by Smith [58] the concurrence defined as $\mathcal{C}_{(AB)} = |X|^2 - \sqrt{P_A P_B}$ showing the graph that he also reported.

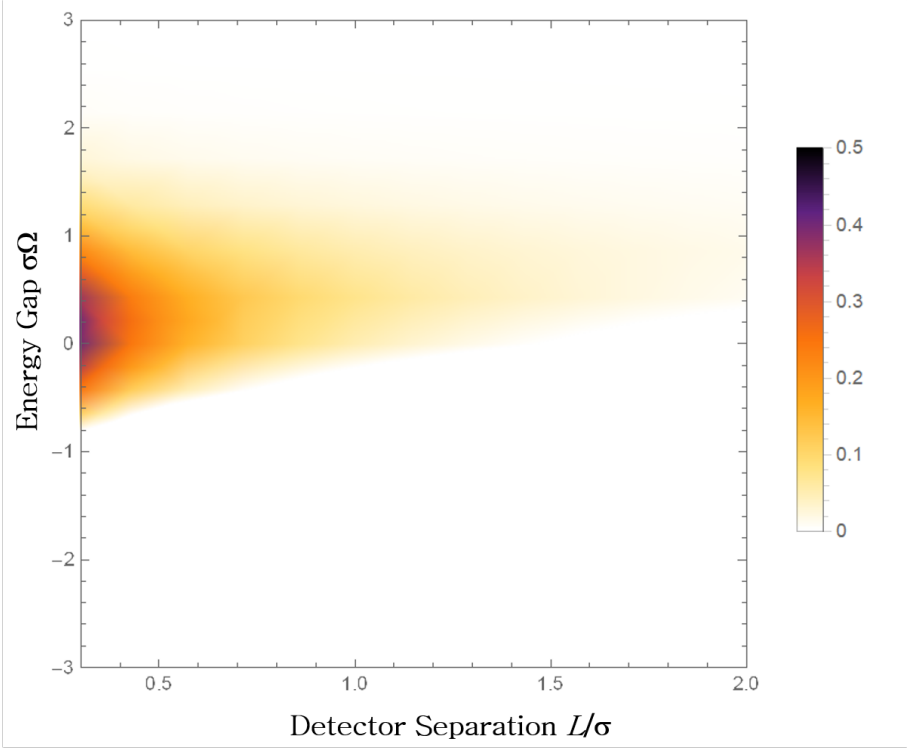

Figure 5.1: Concurrence $\mathcal{C}_{(AB)} = |X|^2 - \sqrt{P_A P_B}$ for the bipartite system derived from the tripartite one

Comparing this results with the work previously obtained by Smith [58] and getting the same behavior of the bipartite system from a tripartite one, we can conclude that the tripartite density matrix we constructed is correct and we can then continue working with it.

5.3 π-tangle

In the following section we present the results for the triangle and linear arrangements obtained by computing the π-tangle entanglement measurement with the density matrix generated in the previous section. Along with the results, the analysis for the unexpected behaviour for both cases and the possible explanations are presented. Furthermore, the analysis for the differences between both arrangements is presented.

5.3.1 Triangle arrangement

The first arrangement we analyze is the triangular one. We start from the easiest system to solve as the distances between the detectors are the same, so the system will acquire a symmetry which will simplify all the followed procedure. Thus, in the present subsection the calculations followed to compute the π-tangle for this type of arrangement and the results for different values for the separation and energy gap are presented.

For the triangle arrangement, we will take into consideration that the energy gap of each detector and distance between them are the same for all. So, the probability of switching from the base state to the excited state for each detector is the same and the matrix elements end up like

$$X_{CB} = X_{CA} = X_{BA} = X \qquad and \qquad C_{BC} = C_{AC} = C_{AB} = C$$

After this change the density matrix becomes

$$\rho_{ABC} = \begin{pmatrix} 1-3P & 0 & 0 & 0 & X & X & X & 0 \\ 0 & P & C & C & 0 & 0 & 0 & 0 \\ 0 & C^* & P & C & 0 & 0 & 0 & 0 \\ 0 & C^* & C^* & P & 0 & 0 & 0 & 0 \\ X^* & 0 & 0 & 0 & 0 & 0 & 0 & 0 \\ X^* & 0 & 0 & 0 & 0 & 0 & 0 & 0 \\ X^* & 0 & 0 & 0 & 0 & 0 & 0 & 0 \\ 0 & 0 & 0 & 0 & 0 & 0 & 0 & 0 \end{pmatrix} \tag{5.3.1.1}$$

Now, to calculate π_A we first need $\mathcal{N}_{A(BC)}$. With the last density matrix 5.3.1.1, the partial

transpose over A can be written as

$$\rho_{ABC}^{T_A} = \begin{pmatrix} 1-3P & 0 & 0 & 0 & X & C^* & C^* & 0 \\ 0 & P & C & X^* & 0 & 0 & 0 & 0 \\ 0 & C^* & P & X^* & 0 & 0 & 0 & 0 \\ 0 & X & X & P & 0 & 0 & 0 & 0 \\ X^* & 0 & 0 & 0 & 0 & 0 & 0 & 0 \\ C & 0 & 0 & 0 & 0 & 0 & 0 & 0 \\ C & 0 & 0 & 0 & 0 & 0 & 0 & 0 \\ 0 & 0 & 0 & 0 & 0 & 0 & 0 & 0 \end{pmatrix} \tag{5.3.1.2}$$

with eigenvalues:

$$e_1 = e_2 = e_3 = 0$$

$$\begin{aligned} e_4 &= \frac{1}{2}\left(-\sqrt{8|C|^2 + 9P^2 - 6P + 4|X|^2 + 1} - 3P + 1\right) \\ &= \mathcal{O}(\lambda^4) \end{aligned} \tag{5.3.1.3}$$

$$\begin{aligned} e_5 &= \frac{1}{2}\left(\sqrt{8|C|^2 + 9P^2 - 6P + 4|X|^2 + 1} - 3P + 1\right) \\ &= 1 - 3P + \mathcal{O}(\lambda^4) \end{aligned}$$

but for e_6, e_7, e_8 we have the three roots of the polynomial:

$$x^3 - 3Px^2 + (-CC^* + 3P^2 - 2XX^*)x - P^3 + CC^*P - CXX^* + 2PXX^* - C^*XX^* = 0 \tag{5.3.1.4}$$

If C is real, then the polynomial in equation 5.3.1.4 becomes:

$$x^3 - 3Px^2 + (-C^2 + 3P^2 - 2X^2)x - P^3 + C^2P - 2CX^2 + 2PX^2 = 0 \tag{5.3.1.5}$$

Which lead our three last eigenvalues to be:

$$e_6 = P + \frac{2}{\sqrt{3}}\sqrt{C^2 + 2|X|^2}\cos\left(\frac{1}{3}\arccos\frac{3\sqrt{3}C|X|^2}{(C^2 + 2|X|^2)^{3/2}}\right) \tag{5.3.1.6}$$

$$e_7 = P - \frac{2}{\sqrt{3}}\sqrt{C^2 + 2|X|^2}\sin\left(\frac{\pi}{6} + \frac{1}{3}\arccos\frac{3\sqrt{3}C|X|^2}{(C^2 + 2|X|^2)^{3/2}}\right) \tag{5.3.1.7}$$

$$e_8 = P - \frac{2}{\sqrt{3}}\sqrt{C^2 + 2|X|^2}\sin\left(\frac{\pi}{6} - \frac{1}{3}\arccos\frac{3\sqrt{3}C|X|^2}{(C^2+2|X|^2)^{3/2}}\right) \tag{5.3.1.8}$$

The resolution of the cubic equation 5.3.1.5 can be found in appendix B.

Whether or not any of these three last roots are negative or not, will depend on the relative sizes of P compared to $\sqrt{C^2 + 2|X|^2}$. For the specific values of P, X and C, it is very difficult to predict if one of the eigenvalues will be negative. With this purpose the eigenvalues can be evaluated with the specific values in the region of interest as presented in figure 5.2.

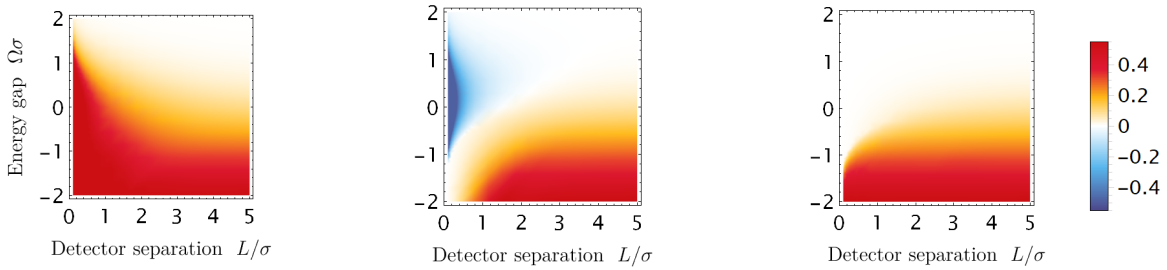

(a) e_6 **(b)** e_7 **(c)** e_8

Figure 5.2: Evaluation of cubic roots a)e_6, b)e_7 and c)e_8 for different values in detector's separation and energy gap.

As it can be seen, the only eigenvalue with a negative region is the one in figure 5.2b. Then, the negative eigenvalue is e_7. Therefore, the Negativity ends up like:

$$\begin{aligned}\mathcal{N}_{A(BC)} &:= \frac{||\rho_{ABC}^{T_A}|| - 1}{2} = \sum_{\lambda_i<0}|\lambda_i| \\ &= max\left[0, \left|P - \frac{2}{\sqrt{3}}\sqrt{C^2+2|X|^2}\sin\left(\frac{\pi}{6} + \frac{1}{3}\arccos\frac{3\sqrt{3}C|X|^2}{(C^2+2|X|^2)^{3/2}}\right)\right|\right] + \mathcal{O}(\lambda^4)\end{aligned} \tag{5.3.1.9}$$

Now, we follow the same procedure to obtain $\mathcal{N}_{A(B)}$ and $\mathcal{N}_{A(C)}$, such as the partial transpose over detector A of ρ_{AB} is

$$\rho_{AB}^{T_A} = \begin{pmatrix} 1-2P & 0 & 0 & C^* \\ 0 & P & X^* & 0 \\ 0 & X & P & 0 \\ C & 0 & 0 & \rho_{77} \end{pmatrix}$$

with eigenvalues

$$e_1 = P - |X| \tag{5.3.1.10}$$

$$e_2 = P + |X| \tag{5.3.1.11}$$

$$\begin{aligned} e_3 &= \frac{1-2P+\rho_{77}}{2} - \sqrt{\left(\frac{1-2P-\rho_{77}}{2}\right)^2 + |C|^2} \\ &= |X|^2 + P^2 + \mathcal{O}(\lambda^6) \end{aligned} \tag{5.3.1.12}$$

$$\begin{aligned} e_4 &= \frac{1-2P+\rho_{77}}{2} + \sqrt{\left(\frac{1-2P-\rho_{77}}{2}\right)^2 + |C|^2} \\ &= 1 - 2P + \mathcal{O}(\lambda^4) \end{aligned} \tag{5.3.1.13}$$

where the only possible negative value is e_1 if $|X|^2 > P^2$. Therefore, the negativity is

$$\mathcal{N}_{A(B)} = \max\left[0, \left|P - |X|\right|\right] \tag{5.3.1.14}$$

The same case happens to $\rho_{AC}^{T_A}$ where its negativity is

$$\mathcal{N}_{A(C)} = \max\left[0, \left|P - |X|\right|\right] \tag{5.3.1.15}$$

Therefore we can calculate:

$$\begin{aligned} \pi_A &= \mathcal{N}^2_{A(BC)} - \mathcal{N}^2_{A(B)} - \mathcal{N}^2_{A(C)} \\ &= \max\left[0, \left|P - \frac{2}{\sqrt{3}}\sqrt{C^2+2|X|^2}\sin\left(\frac{\pi}{6} + \frac{1}{3}\arccos\frac{3\sqrt{3}C|X|^2}{(C^2+2|X|^2)^{3/2}}\right)\right|\right]^2 \\ &\qquad - 2 * \max\left[0, \left|P - |X|\right|\right]^2 \end{aligned} \tag{5.3.1.16}$$

And as π_B and π_c are the same as π_A, we can use the equation for π-tangle and equation 5.3.1.16 to get

$$\begin{aligned} \pi &= \frac{\pi_A + \pi_B + \pi_C}{3} \\ &= \max\left[0, \left|P - \frac{2}{\sqrt{3}}\sqrt{C^2+2|X|^2}\sin\left(\frac{\pi}{6} + \frac{1}{3}\arccos\frac{3\sqrt{3}C|X|^2}{(C^2+2|X|^2)^{3/2}}\right)\right|\right]^2 \\ &\qquad - 2 * \max\left[0, \left|P - |X|\right|\right]^2 \end{aligned} \tag{5.3.1.17}$$

Based on the final π-tangle in equation 5.3.1.17, the results can be plotted in terms of the energy gap ($\Omega\sigma$) and the detector separation (L/σ), as the parameters X, C and P depend in energy gap and separation. In figure 5.3, it can observed that the zone where the values are greater than zero is when the detectors are far apart, contrary to the intuitive idea that as they get closer together there would be more entanglement. This result differs from the bipartite systems where we can find more entanglement when the detectors are closer.

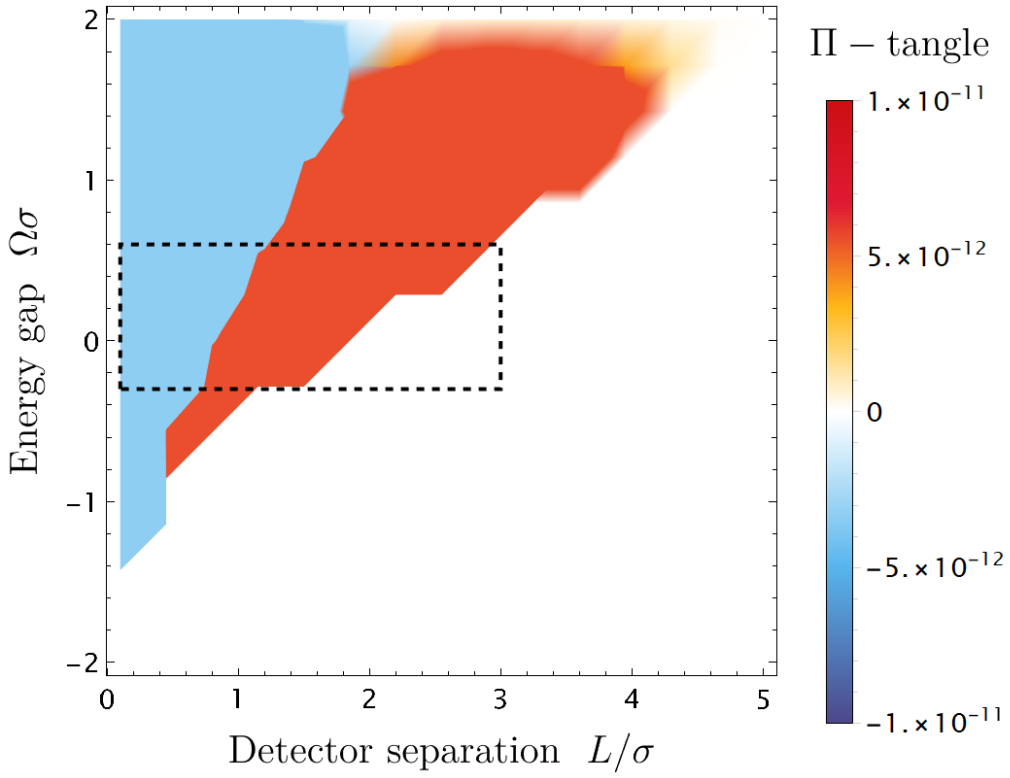

Figure 5.3: Triangle configuration for the evaluation of the π-tangle

The first observation is that there is a sudden change in figure 5.3 between the red and blue regions, and that the color is homogeneous in all of each region. However, zooming into a part of figure 5.4a (marked by the black dotted rectangle), it can be seen that the resolution of the plotting software is not enough to observe all of the values. As we see in figure 5.4, we can choose a value from the energy gap and plot the π-tangle in terms only of the separation of the detectors as in figure 5.4b; in that way we can have more resolution and evaluate where the π-tangle reaches its maximum value.

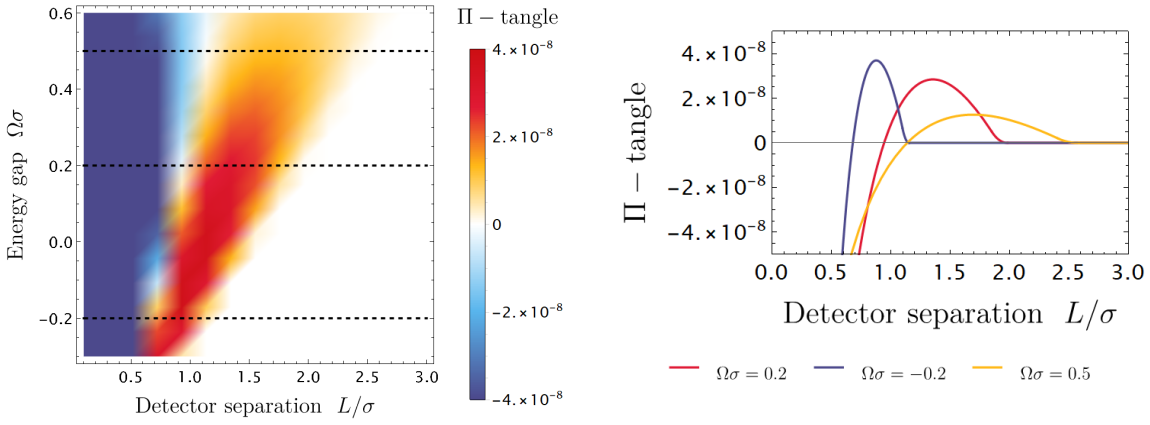

(a) **(b)**

Figure 5.4: Triangle configuration. a) Zoom on the black squared region in figure 5.3. Marked in black pointed lines the three values in b) for the energy gap: $\Omega\sigma = 0.2$ in color red, $\Omega\sigma = -0.2$ in color blue and $\Omega\sigma = 0.5$ in color orange with a maximum value in the π-tangle of $3.69545 * 10^{-8}$ for a constant value of $\Omega\sigma = -0.2$ for energy gap.

Moreover, there is another particularity that does not seem correct: the negative values of the π-tangle. In the publication of Ou and Fan (2007), they prove the general Coffman-Kundu-Wootters (CKW) inequality for tripartite pure and mixed states.

"For any pure $2 \otimes 2 \otimes 2$ states $|\phi\rangle_{ABC}$, the entanglement quantified by the negativity between A and B, between A and C, and between A and the single object BC satisfies the following CKW-inequality-like monogamy inequality:

$$\mathcal{N}_{AB}^2 + \mathcal{N}_{AC}^2 \leq \mathcal{N}_{A(BC)}^2,$$

where $\mathcal{N}_{AB}$ and $\mathcal{N}_{AC}$ are the negativities of the mixed states"[41].

In the work of Ou and Fan, they conclude that the total π-tangle can not be negative as the inequality has to hold. Then the question of what is happening with the values in the negative region on the tripartite case arises. One of the explanations is that the bipartite part is winning over the tripartite part. However, this does not explain the negative values and mathematically it does not hold. In such case, it would be zero and the orange part would be the only one for the tripartite system.

Thus, for this subsection we evaluated the triangle arrangement for three Unruh-DeWitt

detectors. We found that there are some negative values that do not seem to be right based on the work of Ou and Fan on the CWK inequality. Then, the next step to follow is to analyze the values for which the π-tangle is negative.

5.3.2 Analysis of the negative values of the π-tangle

As stated in the previous subsection, we have to analyze the proper values of the π-tangle to see the reason of the behavior in the region in which the values are negative. First, we show the behavior of the X, C and P values to see if we can explain the behavior from there. Next, we expand those variables to evaluate the convergence in the negative region. Finally, we substitute those expansions into the π-tangle to evaluate if it is the problem's origin.

For the individual variables. As it is shown in figure 5.5, in the negative region of the π-tangle, for very small separation, $|X|$ diverge to infinity but P and C converge to one value. On the contrary, for large separation, $|X|$ converge, and, although C diverge, the change is not as quick as $|X|$ in small separation.

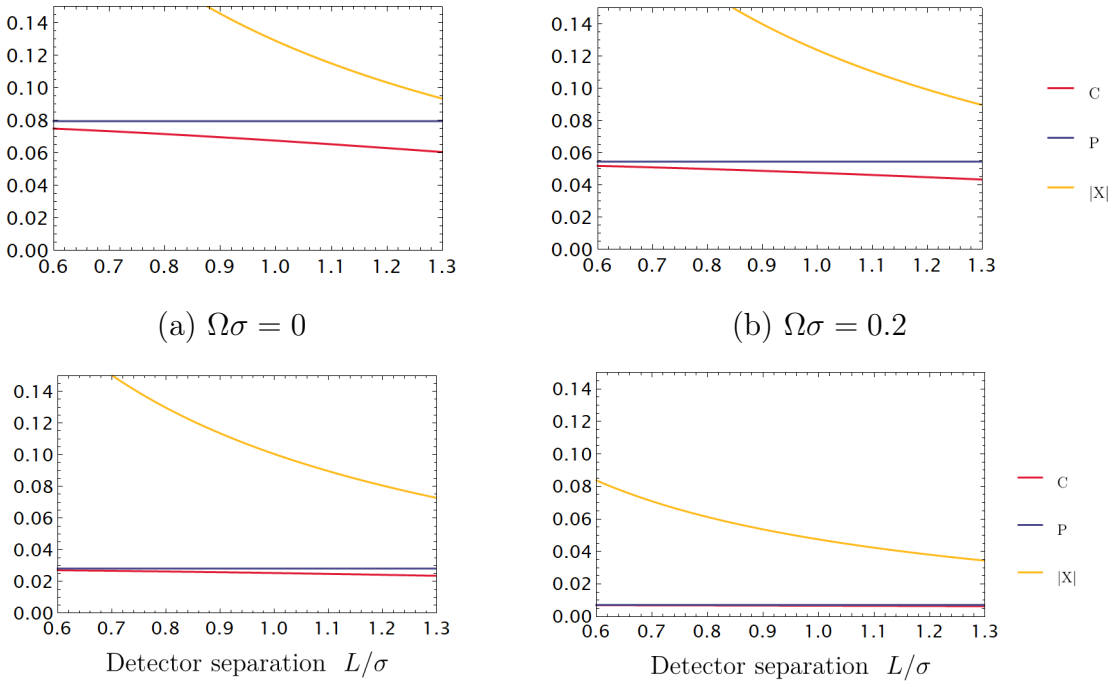

(a) $\Omega\sigma = 0$ (b) $\Omega\sigma = 0.2$

(c) $\Omega\sigma = 0.5$ (d) $\Omega\sigma = 1$

Figure 5.5: Comparison of the specific values of P in blue, C in red and $|X|$ in yellow for different energy gap constant values: a) $\Omega\sigma = 0$; b) $\Omega\sigma = 0.2$; c) $\Omega\sigma = 0.5$; d) $\Omega\sigma = 1$

On the other hand, with the variation in the energy gap ($\Omega\sigma$), the difference between P and C tends to be smaller than the difference between P and X. It is this behavior on $|X|$, which is greater than P and C, that gives us a clue of what is happening to the negative region of the π-tangle. If we see the individual expressions for C, P and X, we can also expand them to analyze their behavior. In the case of C, from equation 5.1.0.10, the expression up to a constant is given by

$$\begin{aligned} C &= \frac{\lambda^2}{4\sqrt{\pi}}\frac{\sigma}{L}e^{-L^2/4\sigma^2}\left(\mathrm{Im}\left[e^{iL\Omega}\,\mathrm{erf}\left(i\frac{L}{2\sigma}+\sigma\Omega\right)\right]-\sin\Omega L\right) \\ &= \frac{\lambda^2}{4\sqrt{\pi}}\frac{\sigma}{L}e^{-L^2/4\sigma^2}\left(-\frac{i\left(e^{iL\Omega}\,\mathrm{erf}\left(i\frac{L}{2\sigma}+\sigma\Omega\right)+e^{-iL\Omega}\,\mathrm{erf}\left(i\frac{L}{2\sigma}-\sigma\Omega\right)\right)}{2}-\sin\Omega L\right) \end{aligned} \tag{5.3.2.1}$$

Then we expand 5.3.2.1 for small L/σ

$$C = \frac{\lambda^2}{4\sqrt{\pi}}\Bigg(\frac{e^{-\sigma^2\Omega^2} + \sigma\Omega\sqrt{\pi}(\mathrm{erf}(\sigma\Omega) - 1)}{\sqrt{\pi}} - \frac{1}{6}\frac{(\sigma^2\Omega^2+1)e^{-\sigma^2\Omega^2} + \sigma\Omega(\sigma^2\Omega^2+\frac{3}{2})(\mathrm{erf}(\sigma\Omega)-1)\sqrt{\pi}}{\sqrt{\pi}}\frac{L^2}{\sigma^2} + \mathcal{O}\Big(\frac{L^3}{\sigma^3}\Big)\Bigg) \tag{5.3.2.2}$$

which is finite, and the leading term is

$$\frac{e^{-\sigma^2\Omega^2} + \sigma\Omega\sqrt{\pi}(\mathrm{erf}(\sigma\Omega) - 1)}{\sqrt{\pi}} \tag{5.3.2.3}$$

Now, we can rewrite P from equation 5.1.0.8 as

$$\begin{aligned} P &= \frac{\lambda^2}{4\pi}\left[e^{-\sigma^2\Omega^2} - \sqrt{\pi}\sigma\Omega\,\mathrm{erfc}(\sigma\Omega)\right] + \mathcal{O}(\lambda^4) \\ &= \frac{\lambda^2\sqrt{\pi}}{4\pi}\left[\frac{e^{-\sigma^2\Omega^2} - \sqrt{\pi}\sigma\Omega\,\mathrm{erfc}(\sigma\Omega)}{\sqrt{\pi}}\right] + \mathcal{O}(\lambda^4) \\ &= \frac{\lambda^2\sqrt{\pi}}{4\pi}\left[\frac{e^{-\sigma^2\Omega^2} + \sigma\Omega\sqrt{\pi}(\mathrm{erf}(\sigma\Omega) - 1)}{\sqrt{\pi}}\right] + \mathcal{O}(\lambda^4) \end{aligned} \tag{5.3.2.4}$$

where its leading order in L/σ is the same as equation 5.3.2.3. As the sub-leading term of C in equation 5.3.2.2 is negative, then we will have $P > C$ at small L/σ, or large X.

Now we can compare those two terms with X rewriting equation 5.1.0.9 and expand it for small L/σ

$$\begin{aligned} X &= i\frac{\lambda^2}{4\sqrt{\pi}}e^{-\sigma^2\Omega^2}\left(\frac{\sigma}{L}e^{-\frac{L^2}{4\sigma^2}}(1 + \mathrm{erf}(\frac{iL}{2\sigma}))\right) \\ &= i\frac{\lambda^2}{4\sqrt{\pi}}e^{-\sigma^2\Omega^2}\left(\frac{\sigma}{L} + \frac{i}{\sqrt{\pi}} - \frac{1}{4}\frac{L}{\sigma} + \mathcal{O}\Big(\frac{L^2}{\sigma^2}\Big)\right) \end{aligned} \tag{5.3.2.5}$$

We note that although P and C do not diverge in the limit where $L \to 0$, X does diverge, which is consistent with the observed in figure 5.5. We now proceed to check this limit for the resulting π-tangle in equation 5.3.1.17.

$$\pi = \Big(\frac{2}{\sqrt{3}}\sqrt{C^2 + 2|X|^2}\sin\left(\frac{\pi}{6} - \frac{1}{3}\arccos\frac{3\sqrt{3}C|X|^2}{(C^2+2|X|^2)^{3/2}}\right) - P\Big)^2 - 2*\Big(|X| - P\Big)^2 \tag{5.3.2.6}$$

$$= \big((-C-2P)\sqrt{2} + 4P\big)\frac{L}{\sigma} + \frac{C^2}{2} - P^2 + PC + \mathcal{O}\Big(\frac{\sigma}{L}\Big) \tag{5.3.2.7}$$

Although $P > C$, it is not guaranteed that $\left(4 - 2\sqrt{2}P\right) > \sqrt{2}C$ for the leading term of the π-tangle to be greater than zero, and that is probably the origin of the negative values we are getting in figure 5.3. If we plot this inequality and compare it to the π-tangle for different values of $\sigma\Omega$ as in figure 5.6, then we realize that when $\sqrt{2}C$ is greater than $\left(4 - 2\sqrt{2}P\right)$ then the π-tangle turns out to be negative in the same limit. This is exactly the reason for the negative behavior of the π-tangle.

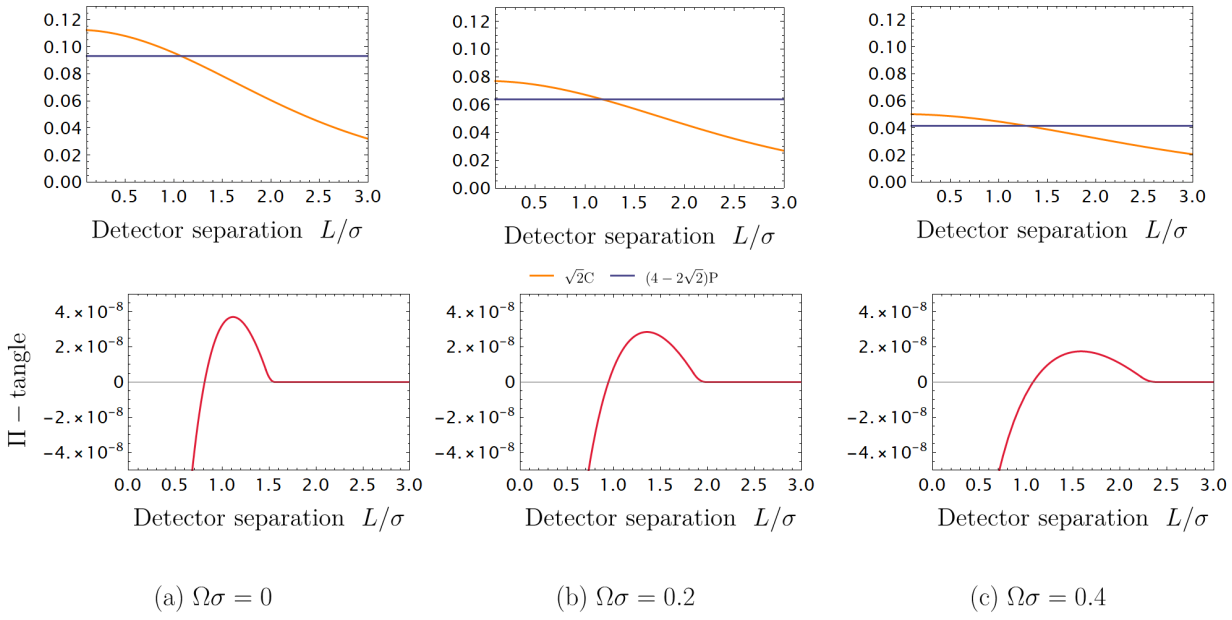

(a) $\Omega\sigma = 0$ (b) $\Omega\sigma = 0.2$ (c) $\Omega\sigma = 0.4$

Figure 5.6: Comparison between $\sqrt{2}C$ in orange, $(4-2\sqrt{2})P$ in blue in the upper graphs and π-tangle in red in the lower graphs for different values of the energy gap: a)$\Omega\sigma = 0$; b)$\Omega\sigma = 0.2$;c)$\Omega\sigma = 0.4$

In this subsection we found the problem's origin for the negative values for the π-tangle which relies in the divergence of the X variable for small separations and its influence on the π-tangle which makes the bipartite subsystems to be greater than the tripartite part. Although we have not found the reason of the influence of this discovery into the final result, we are confident that we are in the right path to give an appropriate explanation.

5.3.3 Analysis of the Perturbation theory

In the previous subsection we found that the divergence of the X parameter for small separation in the π-tangle is the origin of the negative values. Nevertheless, we must explain the reason of

why this is happening and why it is influencing the final result in the tripartite system but it was not an inconvenience for the bipartite system in previous research.

Then, to complete the explanation for the π-tangle's negative values, we have to question if the mathematical approach that we are using is accurate for an exhaustive description of the system. Perturbation theory has been used for the cases in which the system can not be solved analytically. However, it seems that Perturbation Theory is breaking down in the negative region, so we can not trust the π-tangle there. To prove this hypothesis, we have to include the higher terms to evaluate if the values of the π-tangle change in any way. Then, we have to include all the λ^4 terms from the density matrix and the λ^4 eigenvalues. However, as said before, it is very complicated to calculate analytically the rest of the density matrix's terms. Nevertheless, we can include the eigenvalues that did not appear in the negativity although they were negative, such as 5.3.1.3.

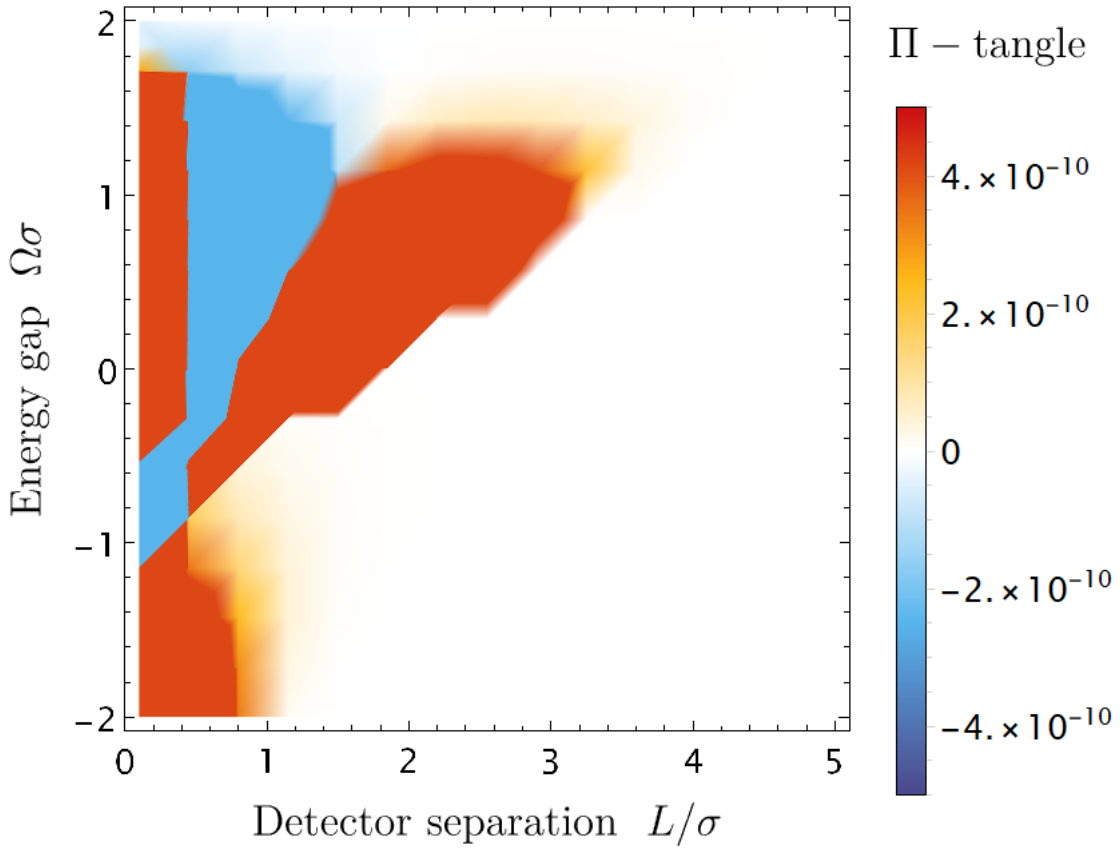

Figure 5.7: Evaluation of the triangle configuration with the extra λ^4 eigenvalue in the Π-tangle

If we include the extra terms, then the π-tangle is now as presented in figure 5.7. As it can be

observed, there is now an additional region with positive values for the π-tangle inside the blue region. With this observation, there is evidence that the Perturbation Theory breaks down in the π-tangle and its negative values can not be trusted. Nevertheless we can trust the positive values when the detectors are far away from each other as the CWK inequality holds and X does not diverge in that region.

Another characteristic we can observe is that the π-tangle maximum is not growing with the addition of the extra term, that would imply that with all the terms, the π-tangle would not be much greater than what we found here.

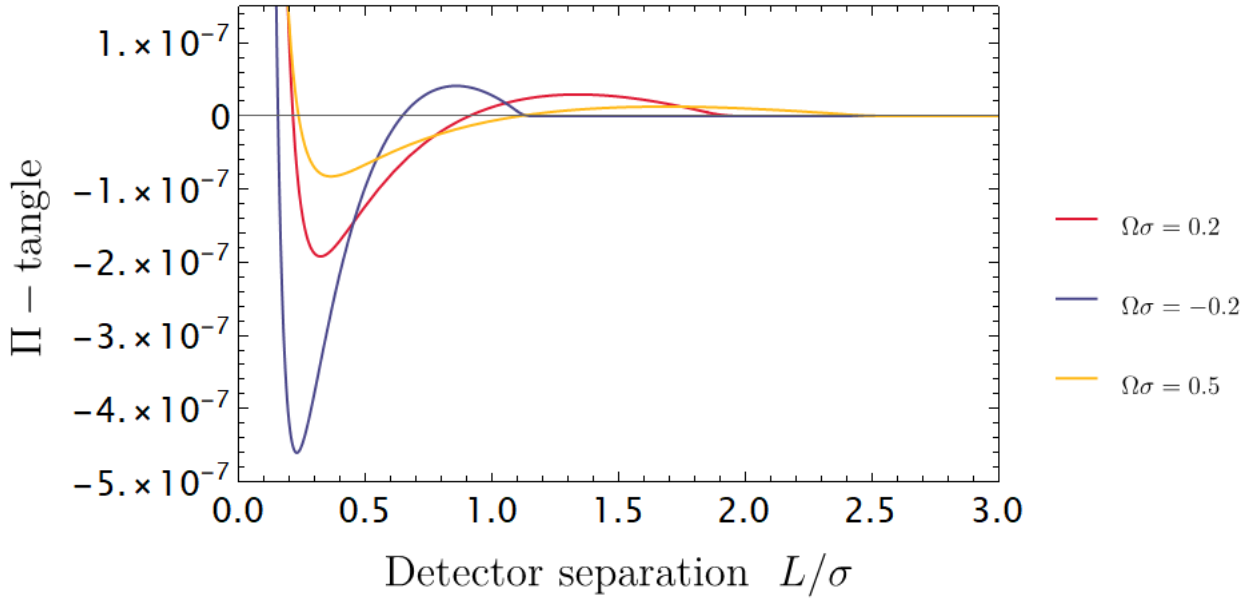

Figure 5.8: 2D plot for the evaluation of the π-tangle for the triangle configuration for three different constant values in the energy gap: $\Omega\sigma = 0.2$ in color red, $\Omega\sigma = -0.2$ in color blue and $\Omega\sigma = 0.5$ in color orange with a maximum value in the π-tangle of $4.1219 * 10^{-8}$ for a constant value of $\Omega\sigma = -0.2$ for energy gap

Presumably, if we continue adding all the parameters we should see an increment in the red region, or if we see figure 5.8, the minimum of the plot would start to change into the positive values. Thus, the reason we do not have a trustful result for the negative values for the π-tangle relies on the limits of Perturbation Theory. We have proved that with the addition of one higher order negative eigenvalue the positive region of the π-tangle increases. However, we can

not predict so far until which point the higher order terms are not going to influence notably anymore in the final result and we will have trustful values.

5.3.4 Aligned arrangement

As we already study the triangle arrangement, the next step to follow is increase the difficulty by changing the initial conditions of the system and compare the results with the ones obtained in the past arrangement. Then, in the present subsection we analyze the next arrangement is when the detectors are aligned in a line. Next we compare it with the triangle case and discuss the similarities and differences and the origin of them.

First of all, the energy gap of each detector is going to prevail the same, however, the separation is not. Hence, the L variable in the matrix elements X and C is going to differ from the previous arrangement, although the probability will prevail the same. So, with this changes, the matrix elements are now

$$X_{CB} = X_{BA} = X_L \qquad and \qquad C_{BC} = C_{AB} = C_L$$

for the two pairs of detectors at the same distance and

$$X_{CA} = X_{2L} \qquad and \qquad C_{AC} = C_{2L}$$

for the last pair of detectors that are positioned at twice the distance.Then the density matrix in equation 5.1.0.11 has now the form

$$\rho_{ABC} = \begin{pmatrix} 1-3P & 0 & 0 & 0 & X_L & X_{2L} & X_L & 0 \\ 0 & P & C_L & C_{2L} & 0 & 0 & 0 & 0 \\ 0 & C_L^* & P & C_L & 0 & 0 & 0 & 0 \\ 0 & C_{2L}^* & C_L^* & P & 0 & 0 & 0 & 0 \\ X_L^* & 0 & 0 & 0 & 0 & 0 & 0 & 0 \\ X_{2L}^* & 0 & 0 & 0 & 0 & 0 & 0 & 0 \\ X_L^* & 0 & 0 & 0 & 0 & 0 & 0 & 0 \\ 0 & 0 & 0 & 0 & 0 & 0 & 0 & 0 \end{pmatrix} \tag{5.3.4.1}$$

Now we can follow the same procedure as before to calculate the π-tangle. To calculate π_A and π_C, that are going to be the same, we need to perform the partial transpose over A (or C) to the matrix in equation 5.3.4.1. Then we will have

$$\rho_{ABC}^{T_A} = \begin{pmatrix} 1-3P & 0 & 0 & 0 & X_L & C_{2L}^* & C_L^* & 0 \\ 0 & P & C_L & X_{2L}^* & 0 & 0 & 0 & 0 \\ 0 & C_L^* & P & X_L^* & 0 & 0 & 0 & 0 \\ 0 & X_{2L} & X_L & P & 0 & 0 & 0 & 0 \\ X_L^* & 0 & 0 & 0 & 0 & 0 & 0 & 0 \\ C_{2L} & 0 & 0 & 0 & 0 & 0 & 0 & 0 \\ C_L & 0 & 0 & 0 & 0 & 0 & 0 & 0 \\ 0 & 0 & 0 & 0 & 0 & 0 & 0 & 0 \end{pmatrix}$$

with eigenvalues:

$$e_1 = e_2 = e_3 = 0 \tag{5.3.4.2}$$

$$\begin{aligned} e_4 &= \frac{1}{2}\left(-\sqrt{1+4C_{2L}^2+4C_L^2-6P+9P^2+4|X_L|^2}-3P+1\right) \\ &= \mathcal{O}(\lambda^4) \end{aligned} \tag{5.3.4.3}$$

$$\begin{aligned} e_5 &= \frac{1}{2}\left(\sqrt{1+4C_{2L}^2+4C_L^2-6P+9P^2+4|X_L|^2}-3P+1\right) \\ &= 1-3P+\mathcal{O}(\lambda^4) \end{aligned} \tag{5.3.4.4}$$

$$e_6 = P + \frac{2}{\sqrt{3}}\sqrt{C_L^2+|X_L|^2+|X_{2L}|^2}\cos\left(\frac{1}{3}\arccos\frac{3\sqrt{3}(C_LX_LX_{2L}^*+C_LX_L^*X_{2L})}{2(C_L^2+|X_L|^2+|X_{2L}|^2)^{3/2}}\right) \tag{5.3.4.5}$$

$$e_7 = P - \frac{2}{\sqrt{3}}\sqrt{C_L^2+|X_L|^2+|X_{2L}|^2} \sin\left(\frac{\pi}{6}+\frac{1}{3}\arccos\frac{3\sqrt{3}(C_LX_LX_{2L}^*+C_LX_L^*X_{2L})}{2(C_L^2+|X_L|^2+|X_{2L}|^2)^{3/2}}\right) \tag{5.3.4.6}$$

$$e_8 = P - \frac{2}{\sqrt{3}}\sqrt{C_L^2+|X_L|^2+|X_{2L}|^2} \sin\left(\frac{\pi}{6}-\frac{1}{3}\arccos\frac{3\sqrt{3}(C_LX_LX_{2L}^*+C_LX_L^*X_{2L})}{2(C_L^2+|X_L|^2+|X_{2L}|^2)^{3/2}}\right) \tag{5.3.4.7}$$

Then, the only possible negative eigenvalue is e_8 in equation 5.3.4.7, so the negativity in equation 4.0.0.15 for subsystem A (and C) is

$$\mathcal{N}_{A(BC)} = \mathcal{N}_{C(AB)} \tag{5.3.4.8}$$

$$= max\left[0, \left|P - \frac{2}{\sqrt{3}}\sqrt{C_L^2 + |X_L|^2 + |X_{2L}|^2}\right.\right. \tag{5.3.4.9}$$

$$\left.\left. \sin\left(\frac{\pi}{6} - \frac{1}{3}\arccos\frac{3\sqrt{3}(C_L X_L X_{2L}^* + C_L X_L^* X_{2L})}{2(C_L^2 + |X_L|^2 + |X_{2L}|^2)^{3/2}}\right)\right|\right] + \mathcal{O}(\lambda^4) \tag{5.3.4.10}$$

In addition, we need the subsystems $\mathcal{N}_{A(B)}$ and $\mathcal{N}_{A(C)}$, which again are equal to $\mathcal{N}_{C(B)}$ and $\mathcal{N}_{C(A)}$, For which we will have the matrices in equations 5.3.4.11 and 5.3.4.17 and their respective eigenvalues

$$\rho_{AB}^{T_A} = \begin{pmatrix} 1-2P & 0 & 0 & C_L* \\ 0 & P & X_L* & 0 \\ 0 & X_L & P & 0 \\ C_L & 0 & 0 & 0 \end{pmatrix} \tag{5.3.4.11}$$

with eigenvalues

$$e_1 = P - |X_L| \tag{5.3.4.12}$$

$$e_2 = P + |X_L| \tag{5.3.4.13}$$

$$e_3 = \frac{1}{2}\left(1 - 2P - \sqrt{1 + 4C_L^2 - 4P + 4P^2}\right) \tag{5.3.4.14}$$

$$= \mathcal{O}(\lambda^4)$$

$$e_4 = \frac{1}{2}\left(1 - 2P + \sqrt{1 + 4C_L^2 - 4P + 4P^2}\right) \tag{5.3.4.15}$$

$$= 1 - 2P + \mathcal{O}(\lambda^4)$$

where the only possible negative value is e_1 in equation 5.3.4.12 if $|X|^2 > P^2$. Therefore, the negativity $\mathcal{N}_{A(B)}$ and $\mathcal{N}_{C(B)}$ is

$$\mathcal{N}_{A(B)} = \mathcal{N}_{C(B)} = \max\left[0, \left|P - |X_L|\right|\right] \tag{5.3.4.16}$$

The same happens to $\mathcal{N}_{A(C)}$ and $\mathcal{N}_{C(A)}$ where we have

$$\rho_{AC}^{T_A} = \begin{pmatrix} 1-2P & 0 & 0 & C_{2L}* \\ 0 & P & X_{2L}* & 0 \\ 0 & X_{2L} & P & 0 \\ C_{2L} & 0 & 0 & 0 \end{pmatrix} \tag{5.3.4.17}$$

with eigenvalues

$$e_1 = P - |X_{2L}| \tag{5.3.4.18}$$

$$e_2 = P + |X_{2L}| \tag{5.3.4.19}$$

$$e_3 = \frac{1}{2}\left(1 - 2P - \sqrt{1 + 4C_{2L}^2 - 4P + 4P^2}\right) \tag{5.3.4.20}$$

$$e_4 = \frac{1}{2}\left(1 - 2P + \sqrt{1 + 4C_{2L}^2 - 4P + 4P^2}\right) \tag{5.3.4.21}$$

Then the negativity is

$$\mathcal{N}_{A(C)} = \mathcal{N}_{C(A)} = \max\left[0, \Big||X_{2L}| - P\Big|\right] \tag{5.3.4.22}$$

Therefore we can calculate:

$$\begin{aligned} \pi_A &= \mathcal{N}_{A(BC)}^2 - \mathcal{N}_{A(B)}^2 - \mathcal{N}_{A(C)}^2 \\ &= \max\left[0, \frac{2}{\sqrt{3}}\sqrt{C_L^2 + |X_L|^2 + |X_{2L}|^2}\sin\left(\frac{\pi}{6} - \frac{1}{3}\arccos\frac{3\sqrt{3}(C_L X_L X_{2L}^* + C_L X_L^* X_{2L})}{2(C_L^2 + |X_L|^2 + |X_{2L}|^2)^{3/2}}\right) - P\right]^2 \\ &\quad - \max\left[0, |X_L| - P\right]^2 - \max\left[0, |X_{2L}| - P\right]^2 \end{aligned} \tag{5.3.4.23}$$

That it is exactly the same as π_C defined as

$$\begin{aligned} \pi_C &= \mathcal{N}_{C(ABC)}^2 - \mathcal{N}_{C(B)}^2 - \mathcal{N}_{C(A)}^2 \\ &= \max\left[0, \frac{2}{\sqrt{3}}\sqrt{C_L^2 + |X_L|^2 + |X_{2L}|^2}\sin\left(\frac{\pi}{6} - \frac{1}{3}\arccos\frac{3\sqrt{3}(C_L X_L X_{2L}^* + C_L X_L^* X_{2L})}{2(C_L^2 + |X_L|^2 + |X_{2L}|^2)^{3/2}}\right) - P\right]^2 \\ &\quad - \max\left[0, |X_L| - P\right]^2 - \max\left[0, |X_{2L}| - P\right]^2 \end{aligned} \tag{5.3.4.24}$$

In the same way we can perform the calculation for π_B which is is going to be different as π_A and π_C as there is a difference in their separations. So now we can calculate π_B with the matrix

in equation 5.3.4.25.

$$\rho_{ABC}^{T_B} = \begin{pmatrix} 1-3P & 0 & 0 & 0 & C_L^* & X_{2L} & C_L & 0 \\ 0 & P & X_L^* & C_{2L} & 0 & 0 & 0 & 0 \\ 0 & X_L & P & X_L & 0 & 0 & 0 & 0 \\ 0 & C_{2L}^* & X_L^* & P & 0 & 0 & 0 & 0 \\ C_L & 0 & 0 & 0 & 0 & 0 & 0 & 0 \\ X_{2L}^* & 0 & 0 & 0 & 0 & 0 & 0 & 0 \\ C_L^* & 0 & 0 & 0 & 0 & 0 & 0 & 0 \\ 0 & 0 & 0 & 0 & 0 & 0 & 0 & 0 \end{pmatrix} \tag{5.3.4.25}$$

which have the eigenvalues:

$$e_1 = e_2 = e_3 = 0 \tag{5.3.4.26}$$

$$\begin{aligned} e_4 &= \frac{1}{2}\left(-\sqrt{1+8C_L^2-6P+9P^2+4|X_{2L}|^2}-3P+1\right) \\ &= 1-3P+\mathcal{O}(\lambda^4) \end{aligned} \tag{5.3.4.27}$$

$$\begin{aligned} e_5 &= \frac{1}{2}\left(\sqrt{1+8C_L^2-6P+9P^2+4|X_{2L}|^2}-3P+1\right) \\ &= \mathcal{O}(\lambda^4) \end{aligned} \tag{5.3.4.28}$$

$$e_6 = P - \frac{2}{\sqrt{3}}\sqrt{C_{2L}^2+2|X_L|^2}\sin\left(\frac{\pi}{6}+\frac{1}{3}\arccos\frac{3\sqrt{3}C_{2L}|X_L|^2}{(C_{2L}^2+2|X_L|^2)^{3/2}}\right) \tag{5.3.4.29}$$

$$e_7 = P - \frac{2}{\sqrt{3}}\sqrt{C_{2L}^2+2|X_L|^2}\sin\left(\frac{\pi}{6}-\frac{1}{3}\arccos\frac{3\sqrt{3}C_{2L}|X_L|^2}{(C_{2L}^2+2|X_L|^2)^{3/2}}\right) \tag{5.3.4.30}$$

$$e_8 = P + \frac{2}{\sqrt{3}}\sqrt{C_{2L}^2+2|X_L|^2}\cos\left(\frac{1}{3}\arccos\frac{3\sqrt{3}C_{2L}|X_L|^2}{(C_{2L}^2+2|X_L|^2)^{3/2}}\right); \tag{5.3.4.31}$$

which give us the negativity:

$$\mathcal{N}_{B(AC)} = \max\left[0, |\frac{C_{2L}}{2}+P-\frac{\sqrt{C_{2L}^2+8|X_L|^2}}{2}|\right]+\mathcal{O}(\lambda^4) \tag{5.3.4.32}$$

For the next values, we could calculate the partial trace of A and C of 5.3.4.25 to realize that those terms are exactly the same as equation 5.3.1.14 and 5.3.1.15, therefore we can calculate:

$$\begin{aligned}\pi_B &= \mathcal{N}^2_{B(AC)} - \mathcal{N}^2_{B(A)} - \mathcal{N}^2_{B(C)} \\ &= \max\left[0, C_{2L} - P + \frac{\sqrt{C_{2L}^2 + 8|X_L|^2}}{2} - \frac{C_{2L}}{2} - P\right]^2 - 2 * \max\left[0, |X_L| - P\right]^2 \end{aligned} \quad (5.3.4.33)$$

Finally, we can use equations 5.3.4.23, 5.3.4.24, 5.3.4.33, and 4.0.0.11 for π-tangle to get

$$\begin{aligned}\pi &= \frac{\pi_A + \pi_B + \pi_C}{3} \\ &= \frac{2}{3}[max\left[0, \frac{2}{\sqrt{3}}\sqrt{C_L^2 + |X_L|^2 + |X_{2L}|^2}\sin\left(\frac{\pi}{6} - \frac{1}{3}\arccos\frac{3\sqrt{3}(C_L X_L X_{2L}^* + C_L X_L^* X_{2L})}{2(C_L^2 + |X_L|^2 + |X_{2L}|^2)^{3/2}}\right) - P\right]^2 \\ &- \max\left[0, |X_L| - P\right]^2 - \max\left[0, |X_{2L}| - P\right]^2] + \\ &\frac{1}{3}\left[max\left[0, C_{2L} - P + \frac{\sqrt{C_{2L}^2 + 8|X_L|^2}}{2} - \frac{C_{2L}}{2} - P\right]^2 - 2 * max\left[0, |X_L| - P\right]^2\right]\end{aligned} \quad (5.3.4.34)$$

With the expression in 5.3.4.34, we can plot it for a range of energy gap ($\Omega\sigma$) and detector separation (L/σ) as in figure 5.9.

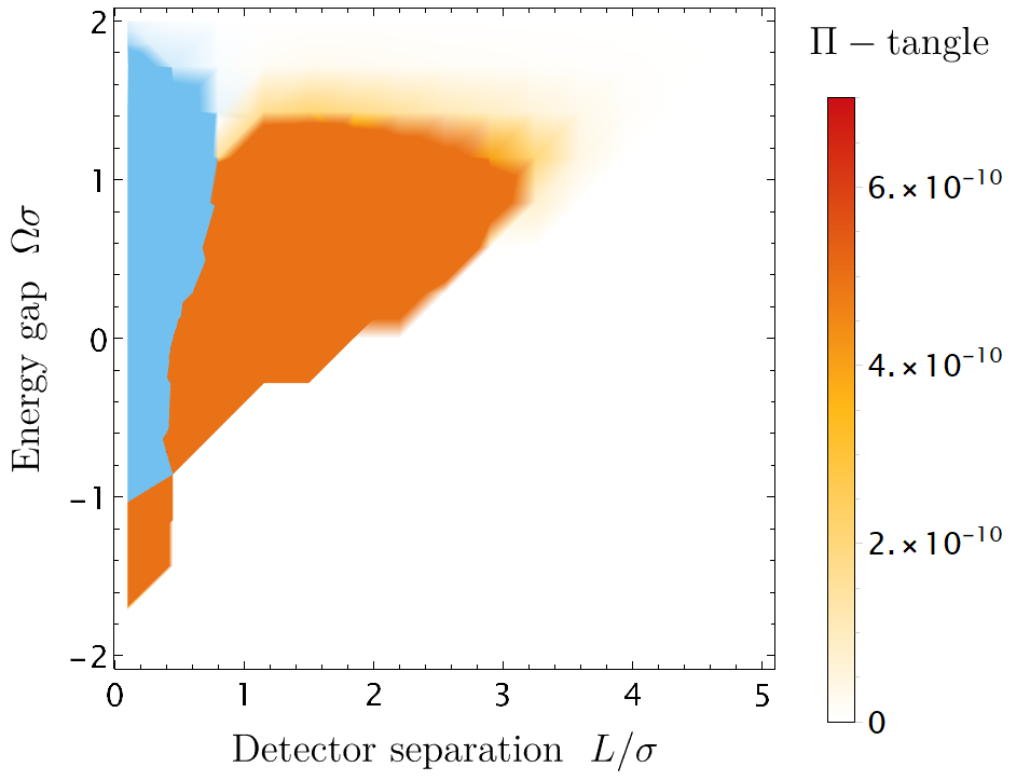

Figure 5.9: Linear configuration for the evaluation of the π-tangle

The behavior we can observe for the linear arrangement is the same as for the triangle case with the same maximum value for the π-tangle and a similar region of negative values. To evaluate if the same explanation of Perturbation Theory breaking down holds, we can add the λ^4 eigenvalues to the final expression and graph it to see the change (figure 5.10).

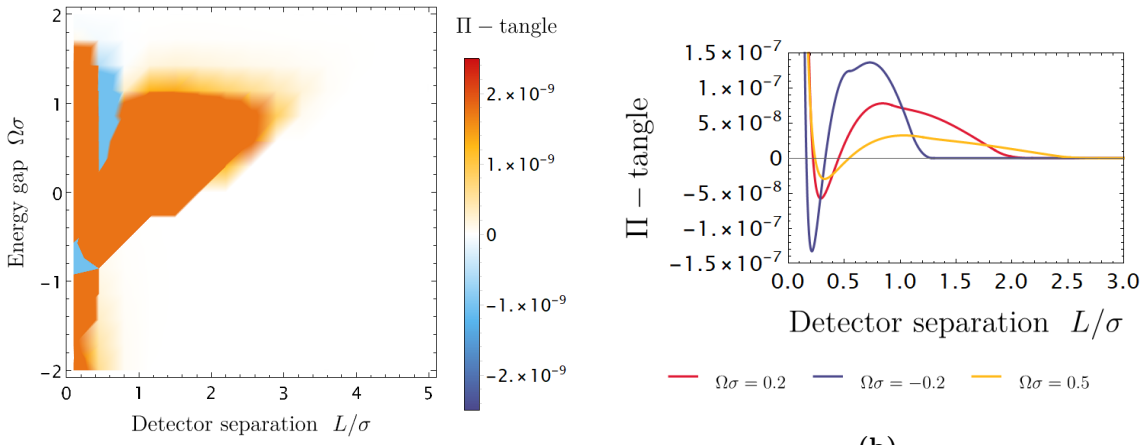

(a) **(b)**

Figure 5.10: Linear configuration of three Unruh-DeWitt detectors for the evaluation of π-tangle with the extra λ^4 eigenvalue with dependency on a) the detector separation (L/σ) and its energy gap ($\Omega\sigma$) and b) detector separation (L/σ) and three different constant vaules for the energy gap: $\Omega\sigma = 0.2$ in color red, $\Omega\sigma = -0.2$ in color blue and $\Omega\sigma = 0.5$ in color orange with a maximum value in the π-tangle of $1.3644 * 10^{-7}$ for a constant value of $\Omega\sigma = -0.2$ for energy gap

In fact, the behavior with the extra term is consistent with the triangle case, which supports the hypothesis that Perturbation Theory is breaking down for small separation and those values can not be trustful.

Although the density plots of both arrangements (fig.5.7 and 5.10a) seems to differ in the separation in which we can harvest entanglement, in the 2-D graphs (fig.5.8 and 5.10b) we can see that the limit in which we have non-zero values is the same for both arrangements.

The maximum value of the pi-tangle in the triangular and linear case differ for the same energy gap, with corresponding values of $4.1219 * 10^{-8}$ for the triangle arrangement, and $1.3644 * 10^{-7}$ for the linear one. These results differ by a 69.8%, which is more than two thirds of the value. By this result, it follows that we can harvest more entanglement from a linear arrangement in comparison to the triangle one. This would open the possibility to think that there is a dependency on the geometry of the detectors, and it is an important point to take into consideration in future work where there is a change in the geometry of the Minkowski spacetime.

As we have the two extremes in the detector's positioning, we can generalize this result for any arrangement that the limit for entanglement harvesting is the same no matter the system's configuration. This generalization could hold as long as the separation between two pairs of detectors is the same.

Now, comparing with the bipartite case, in which the closer the detectors, the bigger the quantity of entanglement. The comparison in the entanglement's quantification has to be through different criteria as the π-tangle does not give us information from the bipartite case. Nevertheless, from figure 5.1 we can see that the general values are around 0.1 which is six times the magnitude order than the maximum value of the linear case. This observation tells us that as it is possible to harvest entanglement from tripartite systems, the quantity of the bipartite part will overcome the tripartite entanglement measurement.

Finally, it is worth to mention that the definition of π-tangle we used was for pure states as the definition for mixed states ρ_{ABC} must be minimized for all possible decomposition, which is extremizing a cost function over all quantum measurements, which in general is difficult and it is a problem that does not have a general solution or methodology to follow for a general state and it is itself an entire problem to solve for any system we work in. Nevertheless, our results are greater or equal than the values for the minimum decomposition. So, the results obtained are still valid for the system.

Chapter 6

Conclusions and future work

The first conclusion we can get is that we can build a general density matrix of a tripartite system coupled with a field from the Unruh-DeWitt time evolution operator expanded with Perturbation Theory. We only need to expand the time evolution operator to the fourth term in order to have all the non-zero matrix elements. Despite the supposition that elements of higher order should not contribute to the final solution, we found we indeed need higher order terms to have non-negative regions of the π-tangle. Yet, we do not know at which order we have to expand the time evolution operator to obtain a trustful π-tangle results for a Gaussian switching function. It is difficult, but not impossible, to calculate higher order matrix elements in order to use them in the eigenvalues. Thus, this is one of the objectives for our future work.

The next conclusion which we can get is that, although the general form of the density plots for the triangle and linear arrangement are similar, there are some particularities in which they differ. First, for the density plots we would think that as the triangle arrangement has a more elongated graph, we can harvest entanglement when the detectors are farther apart than in the linear arrangement. However, in the 2-D graphs we can see that the limit in the separation in which we can harvest entanglement is the same for both arrangements. Second, although we can not harvest entanglement when the detectors are far apart in the linear arrangement, we do have a larger value of the π-tangle than the triangle case. In fact, we can harvest entanglement of 9.5221×10^{-8} more in the linear case than in the triangle one even when we add the λ^4 term with a maximum value of 4.1219×10^{-8} for the triangle case and 1.3644×10^{-7} for the linear

one which is 69.8% bigger. These two situations are important to take into consideration for future works as if the limit in the separation is the same for both arrangements it does not have the same value for the π-tangle which will be fundamental in lab experiments as we need to have the maximum possible value to be able to measure it through physical detectors and have the minimum possible noise.

The next conclusion is that even though the π-tangle seems to be a very good tool to evaluate tripartite mixed states, it only carries information of the tripartite entanglement but does not give information on what is happening with the other bipartite interactions.

In addition to the last conclusions, we can say that even with the problem of the minimum decomposition in the π-tangle definition for mixed states, we can conclude that our results are valid as all the positive values for the π-tangle are greater that any minimum decomposition then, in theory, the actual and precise value of the π-tangle will be less or equal of what we calculated.

We can also conclude that for small detector's separation the X variable grows faster than the other variables which means that the results for the bipartite systems are winning over the tripartite part. This also agrees with the concurrence of the bipartite system in figure 5.1 in which for small separation the values grow to infinity, although it is not the exact same region that fails for the tripartite system, it is also included. It is this result by which we can say that Perturbation Theory is breaking down when we have negative values for the π-tangle. However, if we include higher order terms into the equations, we can see that the values of the π-tangle become positive rather than negative. This tells us that we must include all those higher order matrix elements and eigenvalues that we decided to ignore by the supposition that they do not influence in the final result as it happens with the bipartite case. However, we can not say until which point we need to expand our time evolution operator, matrix elements and eigenvalues to have non-negative values in the entire region.

In addition, we can conclude that even if we add those higher order terms, we will have values around the same magnitude order as we saw that even with the sum of the λ^4 eigenvalue the maximum value did not increased, only we obtained more positive values in the region in which we had negative values for the $\pi - tangle$. Besides, the fact that we can not trust our negative

values for the π-tangle also agrees with the results of Ou and Fan [41] in which the π-tangle can only have positive values for any state.

Also, we can say that it is possible to multipartite entanglement from a quantum vacuum through three Unruh-DeWitt detectors using the π-tangle to quantify the entanglement of two possible detectors arrangements in a flat Minkowski space-time. Although the maximum values are very small comparing to the bipartite case, the values are non-zero which is what we are looking for.

As for what we can say about the theoretical basis, everything was already developed and we did not have the necessity to create something new. Due to the fact that our system was neither a W-state nor a GHZ-state, we achieve to measure the entanglement from a non-trivial state. Besides, the followed methodology was enough to expand it to three detectors and to triumphantly harvest entanglement.

Furthermore, there are still questions to be solve, so the next steps to follow are related to calculate all the matrix elements from the general matrix and evaluate if the π-tangle is worth to be calculated through Perturbation Theory. There are two possibilities: either there is a certain point in the expansion in which the contribution is not considerable; or we can not use Perturbation Theory in this kind of system as it breaks down.

Nevertheless, one of the next steps to follow is to use the Delta switching function instead of the Gaussian one. The advantage is that as the former uses a Dirac's Delta which does not need Perturbation Theory to be calculated as it can be evaluated analytically. However, the mathematical approach is more difficult as there are many possibilities in which the detectors can switch. Besides, previous work by Pozas *et al.*, [60] showed that there can not be entanglement harvesting in a system of two detectors switching with a delta function, but it can exists if one of the detectors switch twice. Then, it will be interesting to evaluate if for three detectors we can harvest entanglement or not.

Finally, the work here presented opens the doors investigate all the previous problems that considered bipartite harvesting and generalize them to the tripartite case, such as, tripartite harvesting near moving mirrors, in curved spacetime, near a black hole, and across the event

horizon as one detector falls in. As we can have different geometries for three detectors, it will be interesting to have more possibilities to see the communication from the detectors through a non-trivial, or flat, spacetime.

Bibliography

[1] Klaus Schwab. *The fourth industrial revolution.* World Economic Forum, 2016, p. 172. ISBN: 9781944835019.

[2] Steven Weinberg. "The Search for Unity : Notes for a History of Quantum Field Theory". In: *The MIT Press on behalf of American Academy of Arts & Sciences Stable* 106.4 (2010), pp. 17–35. URL: http://www.jstor.org/stable/20024506.

[3] Eduarado Martin-Martinez. "Relativistic Quantum Information: developments in Quantum Information in general relativistic scenarios". PhD thesis. 2011, p. 287. arXiv: arXiv:1106.0280v1.

[4] Paul M. Alsing and G. J. Milburn. "Teleportation with a Uniformly Accelerated Partner". In: *Physical Review Letters* 91.18 (Oct. 2003). ISSN: 1079-7114. DOI: 10.1103/physrevlett.91.180404. URL: http://dx.doi.org/10.1103/PhysRevLett.91.180404.

[5] Stephen Hawking, Juan Maldacena, and Andrew Strominger. "DeSitter entropy, quantum entanglement and ADS/CFT". In: *Journal of High Energy Physics* 05 (2001).

[6] Eduardo Martín-Martínez and Nicolas C. Menicucci. "Entanglement in curved spacetimes and cosmology". In: *Classical and Quantum Gravity* 31.21 (2014). ISSN: 13616382. DOI: 10.1088/0264-9381/31/21/214001. arXiv: 1408.3420.

[7] Teng Ma and Shao-Ming Fei. "Three-tangle and Three-π for a class of tripartite mixed states". In: (2013), pp. 1–10. DOI: 10.1142/9789814460026_0036. arXiv: 1305.2264. URL: http://arxiv.org/abs/1305.2264%0Ahttp://dx.doi.org/10.1142/9789814460026_0036.

[8] Gheorghe S. Paraoanu. "The Quantum Vacuum". In: *Boston Studies in the Philosophy and History of Science*. Vol. 313. 2015, pp. 181–197. DOI: 10.1007/978-3-319-16655-1_12. arXiv: 1402.1087.

[9] Albert Einstein. "Relativity and the Problem of Space". In: *Relativity: The special and the general theory*. 15th editi. New York: Three Rivers Press, 1961.

[10] Otfried Gühne and Géza Tóth. "Entanglement detection". In: *Physics Reports* 474.1-6 (2009), pp. 1–75. ISSN: 03701573. DOI: 10.1016/j.physrep.2009.02.004. arXiv: 0811.2803.

[11] G. Benenti et al. *Principles of Quantum Computation and Information: A Comprehensive Textbook*. World Scientific Publishing Company Pte. Limited, 2019. ISBN: 9789813279995. URL: https://books.google.com.mx/books?id=3%5C_TcvgEACAAJ.

[12] Xin Wang and Mark M. Wilde. "Cost of Quantum Entanglement Simplified". In: *Physical Review Letters* 125.4 (2020), pp. 32–34. ISSN: 10797114. DOI: 10.1103/PhysRevLett.125.040502. arXiv: 2007.14270.

[13] J. R. Lucas. "The Special and General Theories of Relativity". In: *A Treatise on Time and Space* (2018), pp. 236–241. DOI: 10.4324/9780429401244-47.

[14] Albert Einstein. "The Lorentz Transformation". In: *Relativity: The special and general theory, by Albert Einstein. Translated by Robert W. Lawson.* New York: Henry Holt and Company, 1920. Chap. XI. ISBN: 1-58734-092-5.

[15] Gary William Gibbons. *Relativistic mechanics*. 2016. DOI: 10.1142/9789812815958_0007. URL: https://www.britannica.com/science/relativistic-mechanics.

[16] Antony Valentini. "Non-local correlations in quantum electrodynamics". In: *Physics Letters A* 153.6-7 (1991), pp. 321–325. ISSN: 03759601. DOI: 10.1016/0375-9601(91)90952-5.

[17] Benni Reznik. "Entanglement from the vacuum". In: *Foundations of Physics* 33.1 (2003), pp. 167–176. ISSN: 00159018. DOI: 10.1023/A:1022875910744. arXiv: 0212044 [quant-ph].

[18] Benni Reznik, Alex Retzker, and Jonathan Silman. "Violating Bell's inequalities in vacuum". In: *Physical Review A - Atomic, Molecular, and Optical Physics* 71.4 (2005), pp. 1–4. ISSN: 10502947. DOI: 10.1103/PhysRevA.71.042104. arXiv: 0310058 [quant-ph].

[19] Sho Onoe et al. "Realizing an Unruh-DeWitt detector through electro-optic sampling of the electromagnetic vacuum". In: (2021), pp. 1–23. arXiv: 2103.14360. URL: http://arxiv.org/abs/2103.14360.

[20] Ryszard Horodecki et al. "Quantum entanglement". In: *Reviews of Modern Physics* 81.2 (2009), pp. 865–942. ISSN: 00346861. DOI: 10.1103/RevModPhys.81.865. arXiv: 0702225 [quant-ph].

[21] Asher Peres. "Separability criterion for density matrices". In: *Physical Review Letters* 77.8 (1996), pp. 1413–1415. ISSN: 10797114. DOI: 10.1103/PhysRevLett.77.1413. arXiv: 9604005 [quant-ph].

[22] H. A. Carteret, A. Higuchi, and A. Sudbery. "Multipartite generalization of the Schmidt decomposition". In: *Journal of Mathematical Physics* 41.12 (2000), pp. 7932–7939. ISSN: 00222488. DOI: 10.1063/1.1319516. arXiv: 0006125 [quant-ph].

[23] Arun K. Pati. "Existence of the Schmidt decomposition for tripartite systems". In: *Physics Letters, Section A: General, Atomic and Solid State Physics* 278.3 (2000), pp. 118–122. ISSN: 03759601. DOI: 10.1016/S0375-9601(00)00767-2. arXiv: 9911073 [quant-ph].

[24] Grant Salton, Robert B. Mann, and Nicolas C. Menicucci. "Acceleration-assisted entanglement harvesting and rangefinding". In: *New Journal of Physics* 17.June 2012 (2015), pp. 1–17. ISSN: 13672630. DOI: 10.1088/1367-2630/17/3/035001. arXiv: 1408.1395.

[25] Alejandro Pozas-Kerstjens and Eduardo Martín-Martínez. "Harvesting correlations from the quantum vacuum". In: *Physical Review D - Particles, Fields, Gravitation and Cosmology* 92.6 (2015), pp. 1–17. ISSN: 15502368. DOI: 10.1103/PhysRevD.92.064042. arXiv: 1506.03081.

[26] M. Cliche and A. Kempf. "Vacuum entanglement enhancement by a weak gravitational field". In: *Physical Review D - Particles, Fields, Gravitation and Cosmology* 83.4 (2011), pp. 1–6. ISSN: 15507998. DOI: 10.1103/PhysRevD.83.045019. arXiv: 1008.4926.

[27] Wan Cong et al. "Effects of Horizons on Entanglement Harvesting". In: *arXiv* (2020). ISSN: 23318422. arXiv: 2006.01720.

[28] Zhihong Liu, Jialin Zhang, and Hongwei Yu. "Harvesting Entanglement by uniformly accelerated detectors in the presence of a reflecting boundary". In: (2021), pp. 1–14. arXiv: 2101.00114v1.

[29] Kensuke Gallock-Yoshimura, Erickson Tjoa, and Robert B. Mann. "Harvesting Entanglement with Detectors Freely Falling into a Black Hole". In: i (2021). arXiv: 2102.09573. URL: http://arxiv.org/abs/2102.09573.

[30] Dipankar Barman, Subhajit Barman, and Bibhas Ranjan Majhi. "Role of thermal field in entanglement harvesting between two accelerated Unruh-DeWitt detectors". In: (2021), pp. 30–39. arXiv: 2104.11269. URL: http://arxiv.org/abs/2104.11269.

[31] Laura J Henderson et al. "Harvesting entanglement from the black hole vacuum". In: *Classical and Quantum Gravity* 52.12 (2018), pp. 1–6. ISSN: 22147853. DOI: 10.1080/14484846.2018.1432089.

[32] Ariadna J. Torres-Arenas et al. "Tetrapartite entanglement measures of W-Class in noninertial frames". In: *arXiv* (2018). ISSN: 23318422. arXiv: 1810.03951.

[33] Salman Khan, Niaz Ali Khan, and M. K. Khan. "Non-maximal tripartite entanglement degradation of Dirac and scalar fields in non-inertial frames". In: *Communications in Theoretical Physics* 61.3 (2014), pp. 281–288. ISSN: 02536102. DOI: 10.1088/0253-6102/61/3/02. arXiv: 1402.7152.

[34] Mi Ra Hwang, Daekil Park, and Eylee Jung. "Tripartite entanglement in a noninertial frame". In: *Physical Review A - Atomic, Molecular, and Optical Physics* 83.1 (2011), pp. 1–19. ISSN: 10502947. DOI: 10.1103/PhysRevA.83.012111. arXiv: 1010.6154.

[35] C. Sabín and G. García-Alcaine. "A classification of entanglement in three-qubit systems". In: *European Physical Journal D* 48.3 (2008), pp. 435–442. ISSN: 14346060. DOI: 10.1140/epjd/e2008-00112-5. arXiv: 0707.1780.

[36] Peter van der Straten and Harold Metcalf. "The density matrix". In: *Atoms and Molecules Interacting with Light* (2016), pp. 93–104. DOI: 10.1017/cbo9781316106242.007.

[37] Willi-Hans Steeb and Yorick Hardy. "Partial Trace". In: *Problems and Solutions in Quantum Computing and Quantum Information* (2004), pp. 58–65. DOI: 10.1142/9789812562173_0005.

[38] Jonas Maziero. "Computing Partial Transposes and Related Entanglement Functions". In: *Brazilian Journal of Physics* 46.6 (2016), pp. 605–611. ISSN: 16784448. DOI: 10.1007/s13538-016-0460-1. arXiv: 1609.00323.

[39] Eric Chitambar and Gilad Gour. "Quantum resource theories". In: *Reviews of Modern Physics* 91.2 (2019), pp. 1–62. ISSN: 15390756. DOI: 10.1103/RevModPhys.91.025001. arXiv: 1806.06107.

[40] G. Vidal and R. F. Werner. "Computable measure of entanglement". In: *Physical Review A - Atomic, Molecular, and Optical Physics* 65.3 (2002), pp. 1–11. ISSN: 10502947. DOI: 10.1103/PhysRevA.65.032314. arXiv: 0102117 [quant-ph].

[41] Yong Cheng Ou and Heng Fan. "Monogamy inequality in terms of negativity for three-qubit states". In: *Physical Review A - Atomic, Molecular, and Optical Physics* 75.6 (2007), pp. 1–5. ISSN: 10502947. DOI: 10.1103/PhysRevA.75.062308. arXiv: 0702127 [quant-ph].

[42] Tom Lancaster and Stephen Blundell, Stephen J. Blundell. *Quantum Field Theory for the Gifted Amateur*. Oxford University Press, 2014, p. 485. ISBN: 9780199699322,0199699321.

[43] Allison Sachs. "Entanglement Harvesting and Divergences in Unruh-DeWitt Detector Pairs". PhD thesis. University of Waterloo, 2017, p. 61.

[44] Laura Henderson. "What can detectors detect ?" PhD thesis. University of Waterloo, 2021, p. 152.

[45] Anthony Zee. *Quantum Field Theory in a Nutshell*. Second Edi. Princeton University Press, 2010, p. 576. ISBN: 9780691140346.

[46] R. Frederick Streater. "Wightman quantum field theory". In: *Scholarpedia* 4.5 (2009). revision #190167, p. 7123. DOI: 10.4249/scholarpedia.7123.

[47] William Gordon Ritter. "A General Theory of Wightman Functions". In: 02138 (2004), pp. 1–33. arXiv: 0404027 [math-ph]. URL: http://arxiv.org/abs/math-ph/0404027.

[48] Léon Van Hove. "Von Neumann ' s contribuions to Quantum Theory". In: *American Mathematical Society* (1957), pp. 95–99.

[49] Aram A. Saharian. "Wightman function and vacuum fluctuations in higher dimensional brane models". In: *Physical Review D - Particles, Fields, Gravitation and Cosmology* 73.4 (2006). ISSN: 15507998. DOI: 10.1103/PhysRevD.73.044012. arXiv: 0508038v2 [arXiv:hep-th].

[50] Stephen J. Summers and Reinhard Werner. "Bell's inequalities and quantum field theory. I. General setting". In: *Journal of Mathematical Physics* 28.10 (1987), pp. 2440–2447. ISSN: 00222488. DOI: 10.1063/1.527733.

[51] Stephen J. Summers and Reinhard Werner. "Bell's inequalities and quantum field theory. II. Bell's inequalities are maximally violated in the vacuum". In: *Journal of Mathematical Physics* 28.10 (1987), pp. 2448–2456. ISSN: 00222488. DOI: 10.1063/1.527734.

[52] Greg Ver Steeg and Nicolas C. Menicucci. "Entangling power of an expanding universe". In: *Physical Review D - Particles, Fields, Gravitation and Cosmology* 79.4 (2009), pp. 1–5. ISSN: 15507998. DOI: 10.1103/PhysRevD.79.044027. arXiv: 0711.3066.

[53] Eduardo Martín-Martínez, Alexander R.H. Smith, and Daniel R. Terno. "Spacetime structure and vacuum entanglement". In: *Physical Review D* 93.4 (2016), pp. 1–12. ISSN: 24700029. DOI: 10.1103/PhysRevD.93.044001. arXiv: 1507.02688.

[54] Carlos Sabín et al. "Extracting past-future vacuum correlations using circuit QED". In: *Physical Review Letters* 109.3 (2012), pp. 1–5. ISSN: 00319007. DOI: 10.1103/PhysRevLett.109.033602.

[55] Andrei Tokmakoff. *5.74 Introductory Quantum Mechanics II*. 2009. DOI: 10.1016/S1079-4050(05)80006-7. (Visited on 03/09/2021).

[56] Leonard Mandel and Emil Wolf. *Optical Coherence and Quantum Optics*. Cambridge University Press, 1995, p. 1190. ISBN: 9781139644105. DOI: https://doi.org/10.1017/CBO9781139644105.

[57] Inc. Wolfram Research. *Mathematica, Version 12.2*. Champaign, IL, 2020. URL: https://www.wolfram.com/mathematica.

[58] Alexander R.H. Smith. "Detectors, Reference Frames, and Time". PhD thesis. University of Waterloo, 2017. URL: https://uwspace.uwaterloo.ca/handle/10012/12618.

[59] J. Silman and B. Reznik. "Three-region vacuum nonlocality". In: *arXiv: Quantum Physics* (2005).

[60] Alejandro Pozas-Kerstjens, Jorma Louko, and Eduardo Martín-Martínez. "Degenerate detectors are unable to harvest spacelike entanglement". In: *Physical Review D* 95.10 (2017), pp. 1–10. ISSN: 24700029. DOI: 10.1103/PhysRevD.95.105009. arXiv: 1703.02982.

Appendix A

Time evolution operator

$$
\begin{aligned}
U =& Texp[-i\int dt(\frac{d\tau_A}{dt}H_A[\tau_A(t)+\frac{d\tau_B}{dt}H_B[\tau_B(t)]+\frac{d\tau_C}{dt}H_C[\tau_C(t))] \\
=& 1-i\int dt(\frac{d\tau_A}{dt}H_A[\tau_A(t)+\frac{d\tau_B}{dt}H_B[\tau_B(t)]+\frac{d\tau_C}{dt}H_C[\tau_C(t))] \\
&-\frac{1}{2}\int dtdt'T[\frac{d\tau_A}{dt}\frac{d\tau_A}{dt'}H_A[\tau_A(t)]H_A[\tau_A(t')] \\
&+\frac{d\tau_B}{dt}\frac{d\tau_B}{dt'}H_B[\tau_B(t)]H_B[\tau_B(t')]+\frac{d\tau_C}{dt}\frac{d\tau_C}{dt'}H_C[\tau_C(t)]H_C[\tau_C(t')] \\
&+\frac{d\tau_A}{dt}\frac{d\tau_B}{dt'}H_A[\tau_A(t)]H_B[\tau_B(t')]+\frac{d\tau_A}{dt}\frac{d\tau_C}{dt'}H_A[\tau_A(t)]H_C[\tau_C(t')] \\
&+\frac{d\tau_B}{dt}\frac{d\tau_A}{dt'}H_B[\tau_B(t)]H_A[\tau_A(t')]+\frac{d\tau_B}{dt}\frac{d\tau_C}{dt'}H_B[\tau_B(t)]H_C[\tau_C(t')] \\
&+\frac{d\tau_C}{dt}\frac{d\tau_A}{dt'}H_C[\tau_C(t)]H_A[\tau_A(t')]+\frac{d\tau_C}{dt}\frac{d\tau_B}{dt'}H_C[\tau_C(t)]H_B[\tau_B(t')]] \\
&+\frac{i}{6}\int dtdt'dt''T[\frac{d\tau_A}{dt}\frac{d\tau_A}{dt'}\frac{d\tau_A}{dt''}H_A[\tau_A(t)]H_A[\tau_A(t')]H_A[\tau_A(t'')] \\
&+\frac{d\tau_B}{dt}\frac{d\tau_B}{dt'}\frac{d\tau_B}{dt''}H_B[\tau_B(t)]H_B[\tau_B(t')]H_B[\tau_B(t'')] \\
&+\frac{d\tau_C}{dt}\frac{d\tau_C}{dt'}\frac{d\tau_C}{dt''}H_C[\tau_C(t)]H_C[\tau_C(t')]H_C[\tau_C(t'')] \\
&+\frac{d\tau_A}{dt}\frac{d\tau_A}{dt'}\frac{d\tau_B}{dt''}H_A[\tau_A(t)]H_A[\tau_A(t')]H_B[\tau_B(t'')] \\
&+\frac{d\tau_A}{dt}\frac{d\tau_A}{dt'}\frac{d\tau_C}{dt''}H_A[\tau_A(t)]H_A[\tau_A(t')]H_C[\tau_C(t'')] \\
&+\frac{d\tau_A}{dt}\frac{d\tau_B}{dt'}\frac{d\tau_A}{dt''}H_A[\tau_A(t)]H_B[\tau_B(t')]H_A[\tau_A(t'')] \\
&+\frac{d\tau_A}{dt}\frac{d\tau_B}{dt'}\frac{d\tau_B}{dt''}H_A[\tau_A(t)]H_B[\tau_B(t')]H_B[\tau_B(t'')] \\
&+\frac{d\tau_A}{dt}\frac{d\tau_B}{dt'}\frac{d\tau_C}{dt''}H_A[\tau_A(t)]H_B[\tau_B(t')]H_C[\tau_C(t'')]
\end{aligned}
$$

$$
\begin{aligned}
&+ \frac{d\tau_A}{dt}\frac{d\tau_C}{dt'}\frac{d\tau_A}{dt''} H_A[\tau_A(t)]H_C[\tau_C(t')]H_A[\tau_A(t'')] \\
&+ \frac{d\tau_A}{dt}\frac{d\tau_C}{dt'}\frac{d\tau_B}{dt''} H_A[\tau_A(t)]H_C[\tau_C(t')]H_B[\tau_B(t'')] \\
&+ \frac{d\tau_A}{dt}\frac{d\tau_C}{dt'}\frac{d\tau_C}{dt''} H_A[\tau_A(t)]H_C[\tau_C(t')]H_C[\tau_C(t'')] \\
&+ \frac{d\tau_B}{dt}\frac{d\tau_A}{dt'}\frac{d\tau_A}{dt''} H_B[\tau_B(t)]H_A[\tau_A(t')]H_A[\tau_A(t'')] \\
&+ \frac{d\tau_B}{dt}\frac{d\tau_A}{dt'}\frac{d\tau_B}{dt''} H_B[\tau_B(t)]H_A[\tau_A(t')]H_B[\tau_B(t'')] \\
&+ \frac{d\tau_B}{dt}\frac{d\tau_A}{dt'}\frac{d\tau_C}{dt''} H_B[\tau_B(t)]H_A[\tau_A(t')]H_C[\tau_C(t'')] \\
&+ \frac{d\tau_B}{dt}\frac{d\tau_B}{dt'}\frac{d\tau_A}{dt''} H_B[\tau_B(t)]H_B[\tau_B(t')]H_A[\tau_A(t'')] \\
&+ \frac{d\tau_B}{dt}\frac{d\tau_B}{dt'}\frac{d\tau_C}{dt''} H_B[\tau_B(t)]H_B[\tau_B(t')]H_C[\tau_C(t'')] \\
&+ \frac{d\tau_B}{dt}\frac{d\tau_C}{dt'}\frac{d\tau_A}{dt''} H_B[\tau_B(t)]H_C[\tau_C(t')]H_A[\tau_A(t'')] \\
&+ \frac{d\tau_B}{dt}\frac{d\tau_C}{dt'}\frac{d\tau_B}{dt''} H_B[\tau_B(t)]H_C[\tau_C(t')]H_B[\tau_B(t'')] \\
&+ \frac{d\tau_B}{dt}\frac{d\tau_C}{dt'}\frac{d\tau_C}{dt''} H_B[\tau_B(t)]H_C[\tau_C(t')]H_C[\tau_C(t'')] \\
&+ \frac{d\tau_C}{dt}\frac{d\tau_A}{dt'}\frac{d\tau_A}{dt''} H_C[\tau_C(t)]H_A[\tau_A(t')]H_A[\tau_A(t'')] \\
&+ \frac{d\tau_C}{dt}\frac{d\tau_A}{dt'}\frac{d\tau_B}{dt''} H_C[\tau_C(t)]H_A[\tau_A(t')]H_B[\tau_B(t'')] \\
&+ \frac{d\tau_C}{dt}\frac{d\tau_A}{dt'}\frac{d\tau_C}{dt''} H_C[\tau_C(t)]H_A[\tau_A(t')]H_C[\tau_C(t'')] \\
&+ \frac{d\tau_C}{dt}\frac{d\tau_B}{dt'}\frac{d\tau_A}{dt''} H_C[\tau_C(t)]H_B[\tau_B(t')]H_A[\tau_A(t'')] \\
&+ \frac{d\tau_C}{dt}\frac{d\tau_B}{dt'}\frac{d\tau_B}{dt''} H_C[\tau_C(t)]H_B[\tau_B(t')]H_B[\tau_B(t'')] \\
&+ \frac{d\tau_C}{dt}\frac{d\tau_B}{dt'}\frac{d\tau_C}{dt''} H_C[\tau_C(t)]H_B[\tau_B(t')]H_C[\tau_C(t'')] \\
&+ \frac{d\tau_C}{dt}\frac{d\tau_C}{dt'}\frac{d\tau_A}{dt''} H_C[\tau_C(t)]H_C[\tau_C(t')]H_A[\tau_A(t'')] \\
&+ \frac{d\tau_C}{dt}\frac{d\tau_C}{dt'}\frac{d\tau_B}{dt''} H_C[\tau_C(t)]H_C[\tau_C(t')]H_B[\tau_B(t'')]] + \mathcal{O}(\lambda^4)]
\end{aligned}
$$

Appendix B

Resolution of the cubic equation

From equation 5.3.1.5

$$x^3 - 3Px^2 + (-C^2 + 3P^2 - 2X^2)x - P^3 + C^2P - 2CX^2 + 2PX^2 = 0 \tag{B.0.0.1}$$

The roots of a cubic equation with the form $ax^3 + bx^2 + cx + d = 0$ are real if the discriminant is proved positive. The discriminant is defined as

$$18abcd - 4b^3d + b^2c^2 - 4ac^3 - 27a^2d^2 \tag{B.0.0.2}$$

Then if we define a, b, c and d as

$$a := 1 \tag{B.0.0.3}$$

$$b := -3P \tag{B.0.0.4}$$

$$c := -C^2 + 3P^2 - 2X^2 \tag{B.0.0.5}$$

$$d := -P^3 + C^2P - 2CX^2 + 2PX^2 \tag{B.0.0.6}$$

where

$$W = (C|X|^2 + |X|^2C^*) \tag{B.0.0.7}$$

$$Y^2 = |C|^2 + 2 * |X|^2 \tag{B.0.0.8}$$

Therefore, the discriminant of equation B.0.0.2 for the cubic equation in 5.3.1.5 becomes

$$\begin{aligned} &108P^3\left(-P^3 + PY^2 - W\right) - 54P\left(3P^2 - Y^2\right)\left(-P^3 + PY^2 - W\right) \\ &\qquad - 27\left(-P^3 + PY^2 - W\right)^2 + 9P^2\left(3P^2 - Y^2\right)^2 - 4\left(3P^2 - Y^2\right)^3 \end{aligned} \tag{B.0.0.9}$$

Which simplifies to

$$-27W^2 + 4Y^6 \tag{B.0.0.10}$$

However, it is not trivial to see if B.0.0.10 is positive or negative. This can be shown as followed. We can write each of the variables in polar form

$$C := C_r e^{iC_a}$$

$$X := X_r e^{iX_a}$$

Then equations B.0.0.7 and B.0.0.8 become

$$W = 2C_r X_r^2 \cos(C_a) \tag{B.0.0.11}$$

$$Y = \sqrt{C_r^2 + 2X_r^2} \tag{B.0.0.12}$$

and the discriminant in equation B.0.0.10 becomes

$$4(C_r^2 + 2X_r^2)^3 - 108C_r^2 X_r^4 \cos^2(C_a) \tag{B.0.0.13}$$

But it is still complicated to evaluate it, so we can simplify it further by writing C_r and X_r in polar form as

$$C_r = r\cos(\theta) \tag{B.0.0.14}$$

$$X_r = \frac{\sqrt{2}}{2} r\sin(\theta) \tag{B.0.0.15}$$

then equations B.0.0.11 and B.0.0.12 becomes:

$$W = r^3 \cos(\theta)\sin^2(\theta)\cos(C_a) \tag{B.0.0.16}$$

$$Y = r \tag{B.0.0.17}$$

and the discriminant is

$$r^6\left(4 - 27\cos^2(C_a)\sin^4(\theta)\cos^2(\theta)\right) \tag{B.0.0.18}$$

It will be positive if the term in brackets is positive. Then, we note that the negative term is largest if $C_a = 0$, hence we need to find the extreme by taking the derivative and set it to zero which is

$$-\frac{27\sin^3(\theta)\cos(\theta)(3\cos^2(\theta) - 1)}{2} \tag{B.0.0.19}$$

and it is clear that the derivative vanishes at $\theta = 0$ or $\theta = \frac{\pi}{2}$ or at $\cos(\theta) = \frac{1}{\sqrt{3}}$. Clearly the first two gives the discriminant 1 and, for the last one, 0 which is not negative.

Now let's simplify the cubic equation 5.3.1.5 using the new variables which gives

$$x^3 - r^2 x - r^3 \cos(\theta)\sin^2(\theta)\cos(C_a) \tag{B.0.0.20}$$

This equation have the form of a depressed cubic $t^3 + pt + q = 0$, whose solutions are

$$2\sqrt{-\frac{p}{3}}\cos\left[\frac{1}{3}\arccos\left(\frac{3q}{2p}\sqrt{-\frac{3}{p}}\right) - \frac{2\pi k}{3}\right] \quad \text{for} \quad k = 0, 1, 2 \tag{B.0.0.21}$$

with $p = -r^2$ and $q = -r^3\cos(\theta)\sin^2(\theta)\cos(C_a)$. Hence the three real roots are

$$R_1 = P + \frac{2}{\sqrt{3}} r \cos\left(\frac{1}{3}\arccos\left(\frac{3\sqrt{3}}{2}\cos(\theta)\sin^2(\theta)\cos(C_a)\right)\right) \tag{B.0.0.22}$$

$$R_2 = P - \frac{2}{\sqrt{3}} r \sin\left(\frac{\pi}{6} + \frac{1}{3}\arccos\left(\frac{3\sqrt{3}}{2}\cos(\theta)\sin^2(\theta)\cos(C_a)\right)\right) \tag{B.0.0.23}$$

$$R_3 = P - \frac{2}{\sqrt{3}} r \sin\left(\frac{\pi}{6} - \frac{1}{3}\arccos\left(\frac{3\sqrt{3}}{2}\cos(\theta)\sin^2(\theta)\cos(C_a)\right)\right) \tag{B.0.0.24}$$

In terms of the original variables X, C and P, we can write the roots as:

$$R_1 = P + \frac{2}{\sqrt{3}}\sqrt{C^2 + 2|X|^2}\cos\left(\frac{1}{3}\arccos\frac{3\sqrt{3}C|X|^2}{(C^2 + 2|X|^2)^{3/2}}\right) \tag{B.0.0.25}$$

$$R_2 = P - \frac{2}{\sqrt{3}}\sqrt{C^2 + 2|X|^2}\sin\left(\frac{\pi}{6} + \frac{1}{3}\arccos\frac{3\sqrt{3}C|X|^2}{(C^2 + 2|X|^2)^{3/2}}\right) \tag{B.0.0.26}$$

$$R_3 = P - \frac{2}{\sqrt{3}}\sqrt{C^2 + 2|X|^2}\sin\left(\frac{\pi}{6} - \frac{1}{3}\arccos\frac{3\sqrt{3}C|X|^2}{(C^2 + 2|X|^2)^{3/2}}\right) \tag{B.0.0.27}$$